POLITECNICO
MILANO 1863

The Rough Heston Model

M.Sc. Thesis of
Molinari Simone

Matr: 863508

Supervisor:
Prof. Barucci Emilio

Programme:
Mathematical Engineering

Department of Mathematics
Politecnico di Milano
2018-2019

Contents

List of Figures

List of Tables

Abstract

From high frequency data, it is evident that log-volatility behaves essentially as a fractional Brownian motion. Because of this, rough volatility models have been recently created, in order to reproduce the historical and the implied volatility behaviour. In particular, we study the rough Heston model and its market foundations. However, this model is no longer Markovian and this feature creates some difficulties when dealing with the derivatives pricing world. The rough model can be derived through a market model based on Hawkes processes. Starting from this approach, we are able to compute the log-price characteristic function in the rough volatility framework. We can obtain the rough Heston characteristic function as a solution of a fractional Riccati equations, but this computation is expensive and it requires advanced numerical methods. This is the reason why we present a Markovian approximation of the rough model, called "lifted Heston model", in order to conciliate the simplicity of the classical Heston model and the precision of the rough one.

Keywords: Stochastic volatility; option pricing; fractional Brownian motion; Heston model; rough volatility; Riccati equations

Sommario

É chiaro dai dati dei mercati ad alta frequenza che il logaritmo della volatilità si comporta essenzialmente come un moto Browniano frazionario. Perciò, per riprodurre il comportamento della volatilità storica e implicita, sono stati creati i modelli a volatilità ruvida. In particolare, analizziamo il modello di Heston ruvido e le sue radici nel mercato. Tuttavia, questo modello non è più Markoviano e questa caratteristica crea dei problemi quando si devono prezzare delle opzioni. Il "rough Heston" può essere derivato attraverso un modello di mercato basato sui processi di Hawkes. Seguendo questo approccio, possiamo trovare la funzione caratteristica del log-price nel contesto della volatilità ruvida. Possiamo ottenere la funzione caratteristica come soluzione di un'equazione di Riccati frazionaria, ma questi calcoli sono dispendiosi e richiedono metodi numerici avanzati. Ecco perchè presentiamo un'approssimazione Markoviana del modello ruvido, chiamata "lifted Heston model", così da conciliare la semplicità del modello di Heston classico con la precisione di quello ruvido.

Parole chiave: volatilità stocastica; prezzare opzioni; moto Browniano frazionario; volatilità ruvida; equazioni di Riccati

Introduction

One dimensional stochastic volatility models are able to capture the price movements on a short time scale, improving the precision of the risk derivatives computation.
One of the most famous models of this type is the Heston model, defined as:

$$\begin{aligned} dS_t &= S_t\sqrt{V_t}dW_t \\ dV_t &= \gamma(\theta - V_t)dt + \gamma\nu\sqrt{V_t}dB_t \\ \rho dt &= \langle dW_t, dB_t\rangle \end{aligned}$$

where S is the asset price, γ, θ and ν are suitable parameters, while W and B are two correlated Brownian motions.
This model is popular among the practitioners because it enjoys a closed form for the characteristic function, allowing fast pricing methods based on the Fourier trasform.
However, one main criticality arises: the Heston model fails in reproducing the at-the-money skew of the implied volatility observed in the market.

The ATM volatility skew is the derivative of the implied volatility with respect to log-strike and it is defined as

$$\psi(\tau) := \Big|\frac{\partial\sigma_{BS}(k,\tau)}{\partial k}\Big|_{k=0}$$

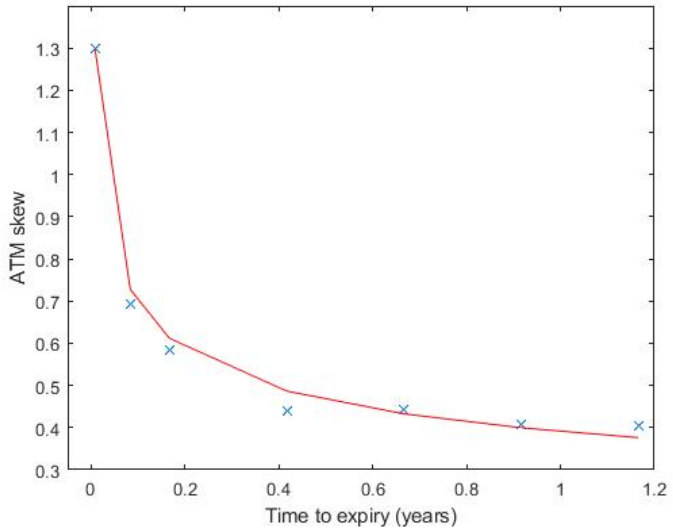

Figure 1: ATM skew of the implied volatility for the FTSE MIB index on October 14, 2014. The real values are the blue cross, while the red curve is the power-law fit $\psi(t) = 0.39 \cdot t^{-0.25}$

In order to fit both the implied and the historical volatility, rough volatility models have been introduced. The price to pay in order to have an higher precision in the derivativatives computation is that these models are no longer Markovian and the volatility process is no more a semi-martingale. This fact makes the pricing and the calibration a difficult task.

Recently, El Euch and Rosenbaum in [9] create a rough "counterpart" of the Heston model, exploiting more advance mathematical tools, such as fractional Brownian motion and fractional integrals.

More precisely, they state this model:

$$dS_t = S_t\sqrt{V_t}dW_t$$
$$V_t = V_0 + \frac{1}{\Gamma(\alpha)}\int_0^t (t-s)^{\alpha-1}\gamma(\theta - V_s)\,ds + \frac{1}{\Gamma(\alpha)}\int_0^t (t-s)^{\alpha-1}\gamma\nu\sqrt{V_s}\,dB_s$$

The additional parameter α belongs to $(1/2, 1)$ and it governs the smoothness of the volatility sample paths. When $\alpha = 1$, we retrieve the classical

Heston model.

The two models share the possibility to compute the log-price characteristic function, which allows the pricing procedure through Fourier methods, but they differ in the fact that the ordinary Riccati equation in the classical Heston is replaced by a fractional equation.
This feature leads to consider the Adams-Bashforth-Moulton algorithm presented in [1] in order to deal with the fractional case. This is a standard numerical method for obtaining solutions of fractional differential equations. However, a large number of steps and computational time are required to achieve satisfactory accuracy.

The justification of the rough model is based on the typical behaviors of market participants at the high frequency scale. A simple microscopic model for an asset price based on Hawkes processes can be built. In this model some of the main features of market microstructure can be encoded: high degree of endogenous orders, no-arbitrage property, buying/selling asymmetry and presence of metaorders. Encoding these features in the model, in the limit an Heston-type model can be obtained, where leverage effect and rough volatility are generated.

Since there are no efficient methods to price derivatives with the rough Heston model, in [6], Abi Jaber and El Euch propose a multi-factor approximation for the rough Heston model, creating the lifted Heston model.
Here, the variance process is built as a weighted sum of n factors driven by the same one-dimensional Brownian motion.

The new model is defined as:

$$dS_t^n = S_t^n \sqrt{V_t^n} dW_t$$
$$V_t^n = g_n(t) + \sum_{1=1}^{n} c_i^n V_t^{n,i}$$

where

$$dV_t^{n,i} = (-\beta_i^n V_t^{n,i} - \gamma V_t^n)dt + \nu\sqrt{V_t^n} dB_t$$
$$g^n(t) = V_0 + \theta \int_0^t K^n(t-s)ds$$

endowed with the initial conditions

$$S_0^n = S_0, \;\; V_0^{n,i} = 0$$

The model is Markovian with respect to the spot price and n variance factors $(V^{n,i})_{1 \leq i \leq n}$.

If we consider the two extreme cases in the multi-factor model, we recover the classical Heston if $n = 1$ and its rough counterpart when n goes to infinity. The lifted model enjoys the best of the two worlds: it can reproduce the ATM skew and it is Markovian. So, we can easily obtain the log-price characteristic function solving a finite system of ordinary Riccati equations.

Finally, Table 1 shows the differences between the tree models.

Characteristics	Heston	Rough Heston	Lifted Heston
Markovianity	✓	✗	✓
Semimartingale	✓	✗	✓
Fit short maturities skew	✗	✓	✓
Characteristic function	Closed	Fractional Riccati	n Riccati
Pricing	Fast	Slow	Fast

Table 1: Summary of the characteristics of the different models

The aim of this thesis is to start from the well-known Heston model and to develop a model which is more realistic from the point of view of the implied volatility.
Starting from the existing literature, we talk about the rough and the lifted Heston model. We aim to resume in one work the three models presented above and to construct an organic *Matlab* code, which allows us to compare the models and to produce a realistic implied volatility surface.

The overall benefit of this work is to create an algorithm that is more precise than the classical Heston one from the implied volatility point of view.
However, this new code doesn't renounce to the feature that has made the previous model very famous among the practitioners: the presence of a

closed-form characteristic function which allows to use fast pricing and calibration methods.

In the last part, in Appendix B, we introduce and explain our attempt to produce a calibration algorithm. Unfortunately, we were not able to obtain satisfactory results. We generally explain how we worked and the encountered criticalities. We describe our starting ideas and we leave our comments as suggestion for future developments.

Our work is organized as follows:

- in chapter 1, we talk about the meaning of the volatility process roughness, defining the general Rough Fractional Stochastic Volatility Model
- in chapter 2, we recall the well-known Heston model
- in chapter 3, we talk about the thesis main focus, the Rough Heston model and how we can construct it starting from the Hawkes processes framework
- in chapter 4, we discuss about the Fourier method for option pricing
- in chapter 5, we describe the numerical methods which allow us to price under the rough Heston model
- in chapter 6, we construct and explain the multi-factor approximation of the rough Heston model

The *Matlab* codes that generates the results described in the thesis are relegated in the Appendix A.
In the Appendix B, we talk about the calibration and the future developments.

Chapter 1

Volatility is rough

1.1 Introduction

In this chapter, we analyze the history of the volatility modeling, starting from the original Black and Scholes work and arriving to the most recent approach, the rough volatility model.
This model involves a sophisticated mathematical tool such as the fractional Brownian motion. We define it and we explain its property.
At the end, we talk about the Rough Fractional Stochastic Volatility model, which is the starting general framework where we can introduce our analysis on rough volatility.

1.2 Volatility modeling

In derivatives world, the most adopted way to model log-price is a continuous semi-martingale (the sum between a local martingale and a finite variation process). Called Y_t the log-price of a given asset, the dynamic takes the form

$$dY_t = \mu(t, Y_t)dt + \sigma(t, Y_t)dW_t$$

where μ is a drift process and W_t is a one-dimensional Brownian motion. The term σ is the volatility process that assumes the most important role in derivatives pricing and hedging.

The first volatility model was produced by Black and Scholes, who considered μ and σ as deterministic constants or as deterministic functions of

time.
This model turned out to be rich of criticalities, in particular it produces prices inconsistent with observed prices for liquid European options. Moreover, benchmark prices are characterized by fat tails and excess kurtosis in return distribution, while the proposed model is not able to show these behaviours.

In order to explain deviation between predicted and real prices, Merton (1976) tried to add jumps in prices dynamics.
After Black and Scholes, Dupire provided a local volatility model, where $\sigma(Y_t, t)$ is a deterministic function of the underliyng price and of the time. Such a model, nevertheless, produces unrealistic dynamics for Y_t and this is a problem when dealing with exotic options.

Another approach is to use the stochastic volatility model: σ is modeled with a continuos Brownian semi-martingale. The most remarkable models are the "Hull and White" and the "Heston".
While stochastic volatility models produce a realistic dynamics, the generated option prices are not consistent with the observed ones.

Nowadays, some models have introduced the local-stochastic volatility in order to enjoy the best of the two worlds. These models can fit the European options market exactly, producing a realistic dynamics for the implied volatility.
The volatility is modeled as the product of a deterministic component $\sigma(S_t, t)$, where S_t is the spot price and a stochastic factor v_t:

$$\begin{aligned} dS_t &= \mu S_t dt + \sqrt{v_t}\sigma(S_t, t) S_t dW_t \\ dv_t &= a(v_t, t)dt + b(v_t, t)dB_t \\ \rho dt &= \mathbb{E}\left[dW_t dB_t\right] \end{aligned}$$

where W and B are two correlated Brownian motions.
The models mentioned above offers two possibilities: regular sample paths or volatility trajectories with regularity close to the Brownian motion one.

Recent high frequency data have highlighted the problem of the smoothness of the volatility.
Gatheral, Jaisson and Rosenbaun in [11] discovered that the log-volatility

behaves as fractional Brownian motion (fBM for short) with Hurst exponent H of order 0.1 at any reasonable time scale (from few days to two years).
This leads them to adopt the fractional stochastic volatility (FSV) model of Comte and Renault [5]. In particular, they were able to reproduce the stylized fact that volatility is a long memory process choosing a fBM with H$>\frac{1}{2}$. Gatheral, Jaisson and Rosenbaun call their model rough fractional stochastic volatility (RSFV) in order to underline that, in contrast to the previous result, H$<\frac{1}{2}$.
RSFV is a particular case of FSV but the key difference is in the choice of H: both in [5] and in [11] authors decided the parameters to fit the volatility skew for small maturities.

1.3 The fractional Brownian motion

Several authors have used fractional Brownian motion to model the volatility regularity. The fBM is a generalization of the classical Brownian motion, but in the former the increments are not independent.
The fBM is a continuous-time centered self-similar Gaussian process indicated as $\left\{W_t^H; t \in \mathbb{R}\right\}$ on $[0,T]$, which starts at zero, has expectation zero for all $t \in [0,T]$, stationary increments and covariance function

$$\mathbb{E}\left[W_t^H W_s^H\right] = \frac{1}{2}\left\{|t|^{2H} + |s|^{2H} - |t-s|^{2H}\right\}$$

where H is a real number in $(0,1)$, called Hurst parameter. This parameter describes the "roughness" of the motion.
For $H = 1/2$, we retrieve the classical Brownian motion.

There are multiple representations of fBm in terms of Brownian motion. The most common is the Mandelbrot-Van Ness representation, where we can build a fractional Brownian motion W^H from a two sided Brownian motion:

$$\begin{aligned} W_t^H = &\frac{1}{\Gamma(H+1/2)} \int_{-\infty}^{0} ((t-s)^{H-1/2} - (-s)^{H-1/2} dW_s + \\ &+ \frac{1}{\Gamma(H+1/2)} \int_0^t (t-s)^{H-1/2} dW_s \end{aligned}$$

The kernel $(t-s)^{H-1/2}$ in the equation above plays the most important role in the rough dynamic. In particular, it is possible to show that the process

$$\int_0^t (t-s)^{H-1/2} dW_s$$

enjoys an Holder regularity $H-\epsilon$ for any $\epsilon > 0$, where H is obviously the Hurst index.

The most important properties of the fractional Brownian motion are listed here:

- For any $t \in \mathbb{R}$, $\Delta \geq 0$, $q > 0$, it holds that:

  $$\mathbb{E}\left[\left|W_{t+\Delta}^H - W_t^H\right|^q\right] = K_q \Delta^{qH}$$

  where K_q is the moment of order q of the absolute value of a standard Gaussian variable.

- Long memory property:

  $$\sum_{k=0}^{\infty} \mathrm{Cov}\left[W_1^H \left(W_k^H - W_{k-1}^H\right)\right] = +\infty \quad \forall H > 1/2$$

  Indeed, $\mathrm{Cov}\left[W_1^H, W_k^H - W_{k-1}^H\right]$ is of order k^{2H-2} as $k \to +\infty$.

- Self-similarity:

  $$W_{at}^H \sim |a|^H W_t^H$$

  This property is due to the fact that the covariance function is homogeneous of order $2H$. Fractional Brownian motion is the only self-similar Gaussian process.

- Stationary increments:

  $$W_t^H - W_s^H \sim W_{t-s}^H$$

  Motion increments on equally long time intervals are identically distributed.

- Dependence of increments:
  Assume that $s_1 < t_1 < s_2 < t_2$

$$\mathbb{E}\left[\left(W_{t_1}^H - W_{s_1}^H\right)\left(W_{t_2}^H - W_{s_2}^H\right)\right] < 0 \text{ for } H \in \left(0, \frac{1}{2}\right)$$
$$\mathbb{E}\left[\left(W_{t_1}^H - W_{s_1}^H\right)\left(W_{t_2}^H - W_{s_2}^H\right)\right] > 0 \text{ for } H \in \left(\frac{1}{2}, 1\right)$$

  Thus, for $H \in (0, 1/2)$, the fBm increments are negatively correlated, while for $H \in (1/2, 1)$, the fBm is persistent.

- Regularity:
  Sample-paths are almost nowhere differentiable. However, almost all trajectories are Holder continuous of any order strictly less than H: for almost each trajectory, for every $T > 0$ and for every $\epsilon > 0$ there exists a constant c such that

$$\left|W_t^H - W_s^H\right| \leq c\,|t - s|^{H-\epsilon}$$

  for $0 < s, t < T$

1.4 The Rough Fractional Stochastic Volatility Model

Statistical tests on high frequency market data support the idea that the that the spot volatility behaves in a way "rougher" than the one previously supposed.
In more recent works, the financial community has started to model the log-volatility dynamics as a fractional Brownian motion W^H with Hurst parameter $H < \frac{1}{2}$.
The models which exploit this approach are called rough volatility models.

One general formulation is:

$$\begin{aligned} dS_t &= \mu S_t dt + \sqrt{\xi_t(t)} S_t dW_t \\ d\xi_t(u) &= \lambda(t, u, \xi_t) dW_t^H \\ \rho dt &= \mathbb{E}\left[dW_t dW_t^H\right] \end{aligned}$$

where, as we said above, W^H is a fractional Brownian motion with $H < \frac{1}{2}$.

Differently from stochastic and local volatility models, the rough one allows to fit both the implied volatility surface and the historical dynamics of volatility.
The most remarkable upgrade of rough world is the fact that the models can reproduce the exploding term structure of the at-the-money skew when maturity goes to zero. The observed term structure of at-the-money volatility skew

$$\psi(\tau) := \left| \frac{\partial \sigma_{BS}(k, \tau)}{\partial k} \right|_{k=0}$$

(the derivative of the implied volatility with respect to log-strike) is well approximated by a power-law function of time to expiry τ. In particular, Fukusawa in [2] discovered that the rough volatility model generates a skew of the form $\psi(\tau) \sim \tau^{H-1/2}$ for small τ.
Usual conventional volatility models produce a term structure that is constant for small τ and similar to a sum of decaying exponential for larger τ.

In this section, we talk about the RFSV (Rough Fractional Stochastic Volatility) defined by Gatheral, Jaisson and Rosenbaum in [11].
Log-volatility shows increments enjoying a scaling property with a constant smoothness parameter. The increments distribution is close to be Gaussian. In [11],the authors suggest the simple model:

$$\log(\sigma_{t+\Delta}) - \log(\sigma_t) = \nu \left(W_{t+\Delta}^H - W_t^H \right) \tag{1.4.1}$$

where W^H is a fractional Brownian motion with Hurst parameter equal to the measured smoothness of the volatility and ν is a positive constant.

An alternative formulation is:

$$\sigma_t = \sigma \exp\left\{ \nu W_t^H \right\}$$

where σ is a positive constant.

The problem of this model is the absence of stationarity, that is a suitable property in order to have a manageable model from the mathematical point of view and to assure a tractable model at very large times.
So it is convenient to impose a fractional Ornstein-Uhlenbeck (fOU for short) dynamics to the log-volatility process with a very long reversion time scale.

A stationary fOU process (X_t) is defined as the stationary solution of the stochastic differential equation

$$dX_t = \nu dW_t^H - \alpha(X_t - m)dt$$

where $m \in \mathbb{R}$, ν and α are positive parameters.
The advantage of Ornstein-Uhlenbeck processes is the presence of an explicit solution:

$$X_t = \nu \int_{-\infty}^{t} e^{-\alpha(t-s)}\, dW_t^H + m \tag{1.4.2}$$

So we have derived the Rough Fractional Stochastic Volatility (RFSV) model for the volatility on the time interval [0,T]:

$$\sigma_t = \exp\{X_t\}, \ t \in [0,T]$$

where X_t satisfies the previous equation for some $\nu > 0$, $\alpha > 0$, $m \in \mathbb{R}$ and $H < 1/2$. This model enjoys stationarity property.
If $\alpha \ll 1/T$, the log-volatility behaves locally (at time scales smaller than T) as a fBM as described by this proposition:

Proposition 1 *Let W^H be a fBM and X^α as in (1.4.2) for a given $\alpha > 0$. As α tends to zero,*

$$\mathbb{E}\left[\sup_{t\in[0,T]} \left|X_t^\alpha - X_0^\alpha - \nu W_t^H\right|\right] \to 0$$

So under the hypothesis $\alpha \ll 1/T$, in RSFV model, the log-volatility process can be considered a fBM.
Setting $\alpha = 0$, we recover the non stationary model (1.4.1) that is equivalent to:

$$X_t - X_s = \nu(W_t^H - W_s^H)$$

Starting from the following corollary, we can deduce that the scaling property of the fBM is approximately reproduced by the fOU process when α is small.

Corollary 1 *Let $q > 0$, $t > 0$, $\Delta > 0$. As α tends to zero, we have*

$$\mathbb{E}\left[\left|X^{\alpha}_{t+\Delta} - X^{\alpha}_{t}\right|^{q}\right] \to \nu^{q} K_{q} \Delta^{qH}$$

where K_q is the moment of order q of the absolute value of a standard Gaussian variable.

The RFSV model is a particular case of FSV model of Comte and Renault [5]. The differences are that in the rough case $H < \frac{1}{2}$ and $\alpha \ll \frac{1}{T}$.
Comte and Renault choose $H > \frac{1}{2}$ in order to obtain long memory and $\frac{1}{T} \ll \alpha$ to obtain a decreasing structure for the volatility skew. The problem is that for short maturities this model generates an inadequate term structure.
In contrast with this fact, opposite choices in RSFV enable to reproduce the observed smoothness for the volatility process and the ATM skew exploding structure.
The parameter $H < \frac{1}{2}$ is also consistent with the "mean reversion" property: if volatility is too high, it tends to decrease and viceversa. On the other hand, α very small allows the log-volatility dynamics to be close to a fBM.

Chapter 2

The Heston model

2.1 Introduction

The Heston model is a one-dimensional stochastic volatility model where the asset price S follows the following dynamic:

$$\begin{aligned} dS_t &= S_t\sqrt{V_t}dW_t \\ dV_t &= \gamma(\theta - V_t)dt + \gamma\nu\sqrt{V_t}dB_t \\ \rho dt &= \langle dW_t, dB_t\rangle \end{aligned}$$

Here the parameters γ, θ, V_0 and ν are positive, while W and B are two correlated Brownian motions.

The popularity of this model is due to three main reasons:

- It can reproduce several important stylized facts of low frequency price data, namely leverage effect, time-varying volatility and fat tails.
- It generates very reasonable shapes and dynamics for the implied volatility surface. Indeed, the "volatility of volatility" parameter ν enables us to control the smile, the correlation parameter ρ to deal with the skew and the initial volatility V_0 fix the at-the-money volatility level. Furthermore, as observed in markets and in contrast to local volatility models, in Heston model, the volatility smile moves in the same direction as the underlying.

- There is an explicit formula for the characteristic function of the asset log-price. From this formula, efficient numerical methods have been developed, allowing for instantaneous model calibration and pricing of derivatives.

In this classical model, the volatility follows a Brownian semi-martingale, while as said in the previous sections the historical volatility of time-series behaves in a rougher way.

2.2 Characteristic function for Heston model

The closed formula for the characteristic function in Heston model is obtained exploiting the Markovianity and the time-homogeneity.
Applying Ito's formula to the function

$$L(t,a,V_t) = \mathbb{E}\left[e^{ia\log(S_T)} \mid \mathcal{F}_t\right],\ \mathcal{F}_t = \sigma(W_s, B_s; s \leq t),\ a \in \mathbb{R}$$

the following Feynman-Kac partial differential equation for L can be derived, since the process L is a martingale:

$$-\partial_t L(t,a,S,V) = (\gamma(\theta - V)\partial_v + \frac{1}{2}(\gamma\nu)^2 V\partial^2_{vv} + \frac{1}{2}S^2V\partial^2_{ss} + \rho\nu\gamma SV\partial^2_{sv})L(t,a,S,V)$$

with boundary condition $L(T,a,S,V) = e^{ia\log(S)}$. From this PDE, we can check that the characteristic function of the log-price $X_t = \log(S_t/S_0)$ satisfies

$$\mathbb{E}\left[e^{iaX_t}\right] = \exp\left(g(a,t) + V_0 h(a,t)\right)$$

where h is the solution of the following Riccati equation:

$$\partial_t h = \frac{1}{2}(-a^2 - ia) + \gamma(ia\rho\nu - 1)h(a,s) + \frac{(\gamma\nu)^2}{2}h^2(a,s),\ h(a,0) = 0$$

and

$$g(a,t) = \theta\gamma\int_0^t h(a,s)\,ds$$

The solution of the Riccati equation leads to a closed-form formula for the characteristic function of the log-price.

Chapter 3

The Rough Heston Model

3.1 Introduction

Our aim is to derive a rough counterpart of the Heston model. The rough Heston model is not Markovian and its variance process is not longer a semi-martingale. So it seems difficult to adapt the classical Heston model to our framework.
The approach proposed in [9] is followed: the microstructural models called Hawkes processes are able to reproduce the stylized facts observed in the high frequency markets and in the long run they show a rough behaviour.
Briefly, a suitable sequence of Hawkes processes can converge to rough Heston model and, in particular, their characteristic functions approximate in the limit the one of the rough Heston model.
We will arrive to a characteristic function for the log-price that exhibits the same structure of the classical Heston model. The only difference is that the Riccati equation will have a fractional counterpart.

However, the solution of the "rough" equation is no longer explicit and we have to find numerical scheme in order to compute it. This is the reason why we solve the fractional Riccati equation thanks to the Adams-Bashforth-Moulton algorithm for first-order equations presented in [1].

Moreover, the microscopic model for the price based on Hawkes process leads to well-known stylized facts of financial data.
The microscopic interactions between agents naturally introduce the lever-

age effect at large time scale. Following the Black's definition, we explain the phenomenon in this way: when the price of an asset is increasing, its volatility drops, while, when it decreases, the volatility tends to become larger.
The rough Heston model, obtained considering the usual behaviour of market partecipants, leads to a price dynamics showing the leverage effect.

3.2 Hawkes processes

A Hawkes process $(N_t)_{t\geq 0}$ is a self-exciting point process, whose intensity at time t, denoted by λ_t, is of the form

$$\lambda_t = \mu + \sum_{0<J_i<t} \phi(t - J_i) = \mu + \int_{(0,t)} \phi(t-s)\, dN_s$$

where μ is a positive real number, ϕ a regression kernel and the J_i are the points (past jumps) of the process before time t.
In recent years, the availability of ultra high-frequency data has made finance one of the main domains of application of Hawkes processes.
They have been introduced in order to study the midquotes prices changes and to estimate the value at risks. More recently, Bacry et al. have developed a microstuctural model for midquote prices based on the difference of two Hawkes processes (see [4]).

Hawkes processes have become popular in price modeling because of two features:

- this type of processes represents a natural extension of Poisson processes.
  Comparing point processes and conventional time series, Poisson processes can be seen as the counterpart of i.i.d. random variables, while Hawkes processes as autoregressive processes.

- the so-called "branching property" gives a practical interpretation to Hawkes processes. Under the assumption $\|\phi\|_1 < 1$, where $\|\phi\|_1$ indicate the L^1 norm of ϕ, Hawkes processes can be represented as a population process where migrants arrive according to a Poisson process with parameter μ.
  Each migrant gives birth to children according to a non-homogeneous

Poisson process with intensity function ϕ. Then this holds for the children, giving birth to their sons according to the same non-homogeneous Poisson process.
Considering the market orders world, migrants can be seen as exogenous orders whereas children are viewed as orders triggered by other orders.

The assumption $\|\phi\|_1 < 1$ is fundamental in order to allow us to follow the population framework. Let us place ourselves in the classical framework where the Hawkes process (N_t) starts at $-\infty$. In that case, if we want to get a stationary intensity with finite first moment, we need the condition $\|\phi\|_1 < 1$. This condition is called stability condition in the Hawkes literature.

$\|\phi\|_1$ (called branching ratio) in a practical approach is used to measure the degree of endogeneity of the market.
The idea is the following: $\|\phi\|_1$ is the average number of children of an individual, $(\|\phi\|_1^2)$ is the average number of grandchildren and so on. All the descendants of a migrant are computed as the average size of its family:

$$\sum_{k\geq 1} \|\phi\|_1^k = \frac{\|\phi\|_1}{(1 - \|\phi\|_1)} \tag{3.2.1}$$

In the financial framework, the proportion of endogenous events is (3.2.1) divided by $1+\|\phi\|_1 /(1 + \|\phi\|_1)$ and, in conclusion, it is equal to $\|\phi\|_1$.

Following [4] and [8], we study the behaviour at large time scales of nearly unstable Hawkes processes (when $\|\phi\|_1$ is close to 1).
We consider a sequence of Hawkes processes observed on $[0, T]$, where T goes to infinity. In the case of a fixed kernel (not depending on T) with norm strictly smaller than one, a deterministic limit for a properly normalized sequence of Hawkes processes can be obtained.

3.3 Rough Fractional Diffusion as scaling limits of nearly unstable Hawkes processes

We consider a sequence of point processes $(N_t^T)_t \geq 0$ indexed by T, where T means T_n with n $\in \mathbb{N}$ tending to infinity.
Fixed T, (N_t^T) satisfies $N_0^T = 0$ and the process is observed on the time interval $[0, T]$. In our framework, we consider the observation scale T going to infinity.

The intensity process (λ_t^T) is defined for $t \geq 0$ by

$$\lambda_t^T = \mu + \sum_{0<J_i<t} \phi^T(t - J_i) = \mu + \int_{(0,t)} \phi^T(t-s)\, dN_s^T$$

where μ is a positive real number and ϕ^T a nonnegative measurable function on $\mathbb{R}^+$ which satisfies $\|\phi\|_1 < +\infty$. For a given T, the process (N_t^T) is defined on a probability space $(\Omega^T, \mathcal{F}^T, \mathbb{P}^T)$ equipped with the filtration $(\mathcal{F}_t^T)_{t\in[0,T]}$, where $\mathcal{F}_t^T$ is a σ-algebra generated by $(N_s^T)_{s\leq t}$. The process N^T is called a Hawkes process.

Let us now give more specific assumptions on the function ϕ^T.

Assumption 1 *For $t \in \mathbb{R}^+$,*

$$\phi^T(t) = a_T \phi(t)$$

where $(a_T)_{T\geq 0}$ is a sequence of positive numbers converging to one such that for all T , $a_T < 1$ and ϕ is a nonnegative measurable function such that

$$\int_0^{+\infty} \phi(s)\, ds = 1 \text{ and } \int_0^{+\infty} s\phi(s)\, ds = m < \infty$$

Moreover, ϕ is differentiable with derivative ϕ' such that $\|\phi'\|_\infty < +\infty$ and $\|\phi'\|_1 < +\infty$.

Under Assumption 1, $\|\phi\|_\infty$ is finite.
Thus, the form of the function ϕ^T depends on T so that its shape is fixed, but its L^1 norm changes with T. For a given T, this L^1 norm is equal to a_T

and it is smaller than one, so the stability condition holds.
Under these hypothesis, we have almost surely no explosion,

$$\lim_{n\to\infty} J_n^T = +\infty$$

However, we do not work in the stationary setting since our process starts at time $t = 0$ and not at $t = -\infty$.

In our framework, two parameters degenerate at infinity: T and $(1 - a_T)^{-1}$. The relationship between these two sequences will determine the scaling behavior of the sequence of Hawkes processes.
Recall that when $\|\phi\|_1$ is fixed and smaller than one, after appropriate scaling, the limit of the sequence of Hawkes processes is deterministic.
In our setting, if $1 - a_T$ tends "slowly" to zero, we can state the following theorem.

Theorem 1 *Assume $T(1 - a_T) \to +\infty$. Then, under Assumption 1, the sequence of Hawkes processes is asymptotically deterministic, in the sense that the following convergence in L^2 holds:*

$$\sup_{v\in[0,1]} \frac{1 - a_T}{T} \left| N_{Tv}^T - \mathbb{E}\left[N_{Tv}^T\right] \right| \to 0$$

On the contrary, if $1 - a_T$ tends too rapidly to zero, the situation is likely to be quite intricate, showing instability even if T is not large enough.

The last case, the most interesting one, is the intermediate case, where $1 - a_T$ tends to zero in such a manner that a nondeterministic scaling limit is obtained, while not being in the preceding degenerate setting.

Let M^T be the martingale process associated to N^T, that is, for $t \geq 0$,

$$M_t^T = N_t^T - \int_0^t \lambda_s^T \, ds$$

We also set ψ_T the function defined on $\mathbb{R}^+$ by

$$\psi_T = \sum_{k=1}^{\infty} (\phi^T)^{*k}(t)$$

where $(\phi^T)^{*1} = \phi^T$ and for $k \geq 2$, $(\phi^T)^{*k}$ denotes the convolution product of $(\phi_T)^{*(k-1)}$ with the function ϕ^T. Note that $\psi^T(t)$ is well defined since $\left\|\phi^T\right\|_1 < 1$.

In the sequel, it will be convenient to work with an other form for the intensity.

Proposition 2 *For all $t \geq 0$, we have*

$$\lambda_t^T = \mu + \int_0^T \psi^T(t-s)\mu\, ds + \int_0^t \psi^T(t-s)\, dM_s^T$$

Now recall that we observe the process (N_t^T) on $[0,T]$. In order to be able to give a proper limit theorem, where the processes live on the same time interval, we rescale our processes so that they are defined on $[0,1]$. We consider for $t \in [0,T]$

$$\lambda_{tT}^T = \mu + \int_0^{tT} \psi^T(Tt-s)\mu\, ds + \int_0^{Tt} \psi^T(Tt-s)\, dM_s^T$$

The multiplicative factor for the space scaling is $(1-a_T)$.
Indeed, in the stationary case, the expectation of λ_t^T is $\mu/(1-\left\|\phi^T\right\|_1)$. Thus the order of magnitude of the intensity is $(1-a_T)^{-1}$. This is the reason why we define

$$C_t^T = \lambda_{tT}^T(1-a_T)$$

The derivation of a suitable scaling limit for renormalized processes is based on the asymptotic behaviour of C_t^T, closely connected to ψ^T.
About ψ^T, the function defined for $x \geq 0$ by

$$\rho^T(x) = T\frac{\psi^T}{\left\|\psi^T\right\|_1}(Tx)$$

is the density of the random variable

$$X^T = \frac{1}{T}\sum_{i=1}^{I^T} X_i$$

where the (X_i) are i.i.d. random variables with density ϕ and I^T is a geometric random variable with parameter $1-a_T$. The characteristic function of the random variable X^T, called $\hat{\rho}^T$, can be defined as

$$\hat{\rho}^T = \frac{1}{i - izm/(T(1-a_T))}$$

Thus, the condition which allows us to obtain a nontrivial limiting law for X^T is that there exist $\lambda > 0$ such that

$$T(1 - a_T) \to \lambda \; as \; T \to +\infty \tag{3.3.1}$$

When this holds, we write $d_0 = m/\lambda$. Consider the following proposition.

Proposition 3 *Assume that (3.3.1) holds. Under Assumption 1, the sequence of random variable X^T converges in law toward an exponential random variable with parameter $1/d_0$.*

Assume from now on that (3.3.1) holds and set $u_T = T(1 - a_T)/\lambda$ (so that u_T tends to one). Proposition 2 is particularly important since it gives us the asymptotic behavior of ψ^T in this setting:

$$\psi^T(Tx) = \rho^T(x)\frac{a_T}{\lambda u_T} \approx \frac{\lambda}{m}e^{-x(\lambda/m)}\frac{1}{\lambda} = \frac{1}{m}e^{-x(\lambda/m)}$$

Let us rewrite the process C_t^T as

$$C_t^T = (1-a_T)\mu + \mu\int_0^t u_T\lambda\psi^T(Ts)\,ds + \int_0^t \sqrt{\lambda}\psi^T(T(t-s))\sqrt{C_s^T}\,dB_s^T \tag{3.3.2}$$

with

$$B_t^T = \frac{1}{\sqrt{T}}\sqrt{u_T}\int_0^{tT}\frac{dM_s^T}{\sqrt{\lambda_s^T}}$$

By observing its quadratic variation, it can be shown that B^T represents a sequence of martingales which converges to a Brownian motion. So, heuristically replacing B^T by a Brownian motion B and $\psi^T(Tx)$ by $\frac{1}{m}e^{-x\lambda/m}$ in (3.3.2),

$$C_t^\infty = \mu(1 - e^{-t(\lambda/m)}) + \frac{\lambda}{m}\int_0^t e^{-(t-s)(\lambda/m)}\sqrt{C_s^\infty}\,dB_s$$

Applying Ito's formula, this gives

$$C_t^\infty = \int_0^t (\mu - C_s^\infty)\frac{\lambda}{m}\,ds + \frac{\lambda}{m}\int_0^t \sqrt{C_s^\infty}\,dB_s$$

which precisely corresponds to the stochastic differential equation satisfied by a CIR process.
Before making the heuristic derivation rigorous, consider an additional assumption.

Assumption 2 *There exists $K_\rho > 0$ such that for all $x \geq 0$ and $T > 0$,*

$$\left|\rho^T(x)\right| < K_\rho$$

Theorem 2 *Assume that (3.3.1) holds. Under Assumptions 1 and 2, the sequence of renormalized Hawkes intensities (C_t^T) converges in law, for the Skorokhod topology, toward the law of the unique strong solution of the following Cox–Ingersoll–Ross stochastic differential equation on $[0, 1]$:*

$$X_t = \int_0^t (\mu - X_s)\frac{\lambda}{m}\, ds + \frac{\sqrt{\lambda}}{m}\int_0^t \sqrt{X_s}\, dB_s$$

Furthermore, the sequence of renormalized Hawkes process

$$V_t^T = \frac{1 - a_T}{T} N_{tT}^T$$

converges in law, for the Skorokhod topology, toward the process

$$\int_0^t X_s\, ds,\ t \in [0, 1]$$

This theorem implies that when $\|\phi\|_1$ is close to 1 and the observation time T is of order $1/(1 - \|\phi\|_1)$, a non degenerate behaviour (neither explosive, nor deterministic) can be obtained for a rescaled Hawkes process.

3.4 Heston model as limit of nearly unstable Hawkes processes

In the previous section, we have studied one-dimensional nearly unstable Hawkes processes. For financial applications, they can, for example, be used to model the arrival of orders in the electronic markets when the number of endogenous orders is much larger than the number of exogenous orders. This framework seems to be very realistic in practice.

In this section, we consider the high-frequency price model which is essentially defined as a difference of two Hawkes processes. We consider a tick-by-tick price model based on a bi-dimensional Hawkes process $N_t = (N_t^+, N_t^-)$, with intensity $\lambda_t = (\lambda_t^+, \lambda_t^-)$ defined by

$$\begin{pmatrix} \lambda_t^+ \\ \lambda_t^- \end{pmatrix} = \begin{pmatrix} \mu_t^+ \\ \mu_t^- \end{pmatrix} + \int_0^t \begin{pmatrix} \phi_1(t-s) & \phi_3(t-s) \\ \phi_2(t-s) & \phi_4(t-s) \end{pmatrix} \begin{pmatrix} dN_s^+ \\ dN_s^- \end{pmatrix}$$

where μ^+ and μ^- are positive constants and

$$\phi = \begin{pmatrix} \phi_1 & \phi_3 \\ \phi_2 & \phi_4 \end{pmatrix} : \mathbb{R}_+ \to \mathcal{M}^2(\mathbb{R}_+^*)$$

is a kernel matrix whose components ϕ_i are positive and locally integrable. Our model for the ultra high frequency transaction price P_t is simply given by

$$P_t = N_t^+ - N_t^-$$

P_t is the price of an asset whose bid-ask spread is almost always equal to one tick and moves by one tick jumps. The tick is defined as the minumum price variation for a financial instrument.

Thus N_t^+ is the number of upward jumps of one tick of the asset in the time interval $[0, t]$ and N_t^- is the number of downward jumps of one tick of the asset in the time interval $[0, t]$.
The instantaneous probability to get an upward (downwards) jump depends on the arrival times of the past upward and downward jumps.

The tick-by-tick model allows us to encode in the model the following stylized facts:

- Markets are highly endogenous (the most of the orders are sent only in order to react to other orders).
- In high frequency markets, there are some mechanisms in order to avoid statistical arbitrage.
- There is an asymmetry on the bid-ask side of order book. For instance, if we consider a market maker with a positive inventory, selling and buying are not the same thing. He prefers to raise the prices following a buy order rather than lower them with the same size sell order. Indeed, its inventory becomes smaller after a buy order, which is a good thing for him, whereas it increases after a sell order. This creates a liquidity asymmetry on the bid and ask sides of the order book.
- The presence of large orders which are split in time by trading algorithms. They are called metaorders.

The first property corresponds to the nearly unstable Hawkes processes framework, while the second and the third impose some conditions on the kernel matrix. Starting from now, a model which encodes all the features presented above is developed.

Let us now interpret the intensity process λ_t^+ (λ_t^- is similar). At time t, the probability to get a new one-tick upward jump between t and $t + dt$ is given by $\lambda_t^+ dt$. This probability can be decomposed into three terms:

- $\mu_+ dt$, which is the Poissonian part of the intensity and corresponds to the probability that the price goes up because of some exogenous reasons
- $\left(\int_0^t \phi_1(t-s)\, dN_s^+\right) dt$, which is the probability of upwards jump induced by past upward jumps
- $\left(\int_0^t \phi_3(t-s)\, dN_s^-\right) dt$, which is the probability of downwards jump induced by past upward jumps

Recalling the markets stylized facts described above, we can encode them from the mathematical point of view in term of Hawkes process parameters. The stylized facts translation in term of parameters can be explained as follows:

- Markets are highly endogenous: as said above, most orders have no real economic motivation and they are sent by algorithms as reaction to other orders. This means that the stability condition for Hawkes processes
$$\mathcal{S}\left(\int_0^{+\infty} a_T \phi(s)\, ds\right) < 1$$
where $\mathcal{S}$ denotes the spectral radius operator, should almost be saturated and that the intensity of exogenous orders, namely μ_T , should be small. In term of model parameters, suitable constraints are therefore
$$a_T \to 1,\ \mathcal{S}\left(\int_0^{+\infty} \phi(s)\, ds\right) = 1,\ \mu_T \to 0$$

- Since it is difficult to make money with high frequency strategies on highly liquid electronic markets, we can state that a "no statistical arbitrage" mechanism is in force. We translate this assuming that, in the long interval, there are on average as many upward than downward jumps. This corresponds to the assumptions
$$\phi_1 + \phi_3 = \phi_2 + \phi_4$$
and
$$\mu^+ = \mu^-$$

- Buying is not the same action as selling (consider the market maker example). This can be modeled in the Hawkes framework assuming that
$$\phi_3 = \beta \phi_2$$
for some $\beta > 1$.

Summarizing, we assume the following structure for the intensity process:

$$\begin{pmatrix} \lambda_t^+ \\ \lambda_t^- \end{pmatrix} = \mu \begin{pmatrix} 1 \\ 1 \end{pmatrix} + \int_0^t \phi(t-s) \cdot \begin{pmatrix} dN_s^+ \\ dN_s^- \end{pmatrix}$$

where

$$\phi = \begin{pmatrix} \phi_1 & \beta\phi_2 \\ \phi_2 & \phi_1 + (\beta - 1)\phi_2 \end{pmatrix}$$

with $\mu > 0$ and $\beta \geq 1$.

Following the intuition in [10], the market endogeneity degree is defined as the spectral radius

$$\mathcal{S}\left(\int_0^{+\infty} \phi(s)\, ds\right) = \|\phi_1\|_1 + \beta \|\phi_2\|_2$$

This spectral radius must be close to unity, but smaller than one.

To respect this assumption, an asymptotic framework can be introduced: in particular, we work in a sequence of probability spaces $(\Omega^T, \mathcal{F}^T, \mathbb{P}^T)$, indexed by $T > 0$, on which $N^T = (N^{T,+}, N^{T,-})$ is a bi-dimensional Hawkes process defined on [0,T] and with intensity

$$\lambda_t^T = \begin{pmatrix} \lambda_t^{T,+} \\ \lambda_t^{T,-} \end{pmatrix} = \mu \begin{pmatrix} 1 \\ 1 \end{pmatrix} + \int_0^t \phi(t-s) \cdot \begin{pmatrix} dN_s^+ \\ dN_s^- \end{pmatrix}$$

Fixed T, the probability space is equipped with the filtration $(\mathcal{F}_t^T)_{t\geq 0}$, where $\mathcal{F}_t^T$ is the σ-algebra generated by $(N_s^T)_{s\leq t}$.
In order to respect all the constraints above, consider this assumption on λ_t^T:

Assumption 3 *We have $\mu_T > 0$ and*

$$\phi^T = a_T \phi \ , \ \phi = \begin{pmatrix} \phi_1 & \beta\phi_2 \\ \phi_2 & \phi_1 + (\beta - 1)\phi_2 \end{pmatrix}$$

where $\beta \geq 1$, ϕ_1 and ϕ_2 are two positive measurable functions such that

$$\mathcal{S}\left(\int_0^{+\infty} \phi(s)\, ds\right) = \|\phi_1\|_1 + \beta \|\phi_2\|_2 = 1$$

and a_T is an increasing sequence of positive numbers converging to one.

Now, we give the convergence result for the microscopic price P^T towards a Heston model. We need two more assumptions:

Assumption 4 *There exist positive parameters λ, μ, and m such that*

$$T(1-a_T) \to_{T\to\infty} \lambda,\ \mu_T = \mu$$

and

$$\mathcal{S}\left(\int_0^{+\infty} x\phi(x)\,dx\right) = m < \infty$$

Assume that the kernel L^1 norm a_T goes to unity in such a way that $T(1-a_T)$ is of order one. This is the only asymptotic framework enabling us to recover a non-degenerate limit. Now let

$$\psi^T = \sum_{k\geq 1} (\phi^T)^{*k}$$

where $(\phi^T)^{*1} = \phi^T$ and for $k > 1$, $(\phi^T)^{*k} = \int_0^t \phi^T(s)(\phi^T)^{*(k-1)}(t-s)\,ds$.

Assumption 5 *The function ψ^T is uniformly bounded and ϕ is differentiable such that each component ϕ_{ij} satisfies $\left\|\phi_{ij}^{'}\right\|_\infty < \infty$ and $\left\|\phi_{ij}^{'}\right\|_1 < \infty$.*

We now state the convergence result, recalling the fact that $\beta > 1$ in order to ensure the liquidity asymmetry which origins of leverage at low frequency.

Theorem 3 *Under Assumptions 3, 4 and 5, as T tends to infinity, the rescaled microscopic price*

$$\frac{1}{T}P_{tT}^T = \frac{N_{tT}^{T,+} - N_{tT}^{T,-}}{T}$$

converges in law for the Skorokhod topology to the following Heston model:

$$P_t = \frac{1}{1 - (\|\phi_1\|)_1 - (\|\phi_2\|)_1}\sqrt{\frac{2}{1+\beta}}\int_0^t \sqrt{X_s}\,dW_s$$

with

$$dX_t = \frac{\lambda}{m}\left(\frac{(\beta+1)\mu}{\lambda} - X_t\right)dt + \frac{1}{m}\sqrt{\frac{1+\beta^2}{1+\beta}}\sqrt{X_t}dB_t,\ X_0 = 0$$

where (W, B) is a correlated bi-dimensional Brownian motion with

$$d\langle W, B\rangle_t = \frac{1-\beta}{\sqrt{2(1+\beta^2)}}dt$$

When $\beta > 1$, the asymmetry in the liquidity generates a negative correlation between low frequency price returns and volatility increments and this is what we call leverage effect.

3.5 Rough Heston model as limit of nearly unstable heavy tailed Hawkes processes

The presence of metaorders on the market is not encoded in the model seen above. This can be translated in the Hawkes framework by adding the condition that the kernel matrix exhibits heavy tails, as observed in practice. Consequently, we need to replace Assumption 4 in order to get a slowly decaying behavior for the kernel matrix. This implies a modification in the asymptotic setting in order to retrieve a non-degenerate scaling limit.
More precisely, Assumption 4 can be substituted with the following one:

Assumption 6 *There exist $\alpha \in (1/2, 1)$ and $C > 0$ such that*

$$\alpha x^\alpha \int_x^\infty \phi_1(s) + \beta\phi_2(s)\, ds \to_{x\to\infty} C$$

Moreover, for some $\lambda^* > 0$ and $\mu > 0$,

$$T^\alpha(1 - a_T) \to_{T\to\infty} \lambda^* > 0,\ T^{1-\alpha}\mu_T \to_{T\to\infty} \mu$$

Note that in practice, estimated values for α are actually close to $1/2$.
We have the following result for the long term limit of our microscopic model:

Theorem 4 *Under Assumptions 3 and 6, as T tends to infinity, the rescaled microscopic price*

$$\sqrt{\frac{1 - a_T}{\mu T^\alpha}} P^T_{tT},\ t \in [0, 1]$$

converges in the sense of finite dimensional laws to the following rough Heston model:

$$P_t = \frac{1}{1 - (\|\phi_1\|)_1 - (\|\phi_2\|)_1} \sqrt{\frac{2}{1+\beta}} \int_0^t \sqrt{Y_s}\, dW_s$$

with Y the unique solution of

$$Y_t = \frac{1}{\Gamma(\alpha)} \int_0^t (t-s)^{\alpha-1} \lambda((1+\beta) - Y_s)\, ds + \frac{1}{\Gamma(\alpha)} \int_0^t (t-s)^{\alpha-1} \lambda\nu \sqrt{Y_s}\, dB_s$$

where (W, B) is a correlated bi-dimensional Brownian motion with correlation

$$\rho = \frac{1-\beta}{\sqrt{2(1+\beta^2)}}$$

and

$$\nu = \sqrt{\frac{2(1+\beta^2)}{\lambda^* \mu (1+\beta)^2}},\ \lambda = \frac{\alpha \lambda^*}{C\Gamma(1-\alpha)}$$

Furthermore, the process Y_t has Holder regularity $\alpha - 1/2 - \epsilon$ for any $\epsilon > 0$.

Comparing this statement with the Theorem 3, we see that the only remarkable difference is the presence of the kernel $(t-s)^{\alpha-1}$ in the two integrals. This is the fractional kernel responsible for the rough behavior of the volatility, where obviously $\alpha - 1/2$ is the Hurst index.

Inspired by this result, our idea is to study the characteristic function of some kind of microscopic price processes in order to deduce the proper one of our rough Heston macroscopic price.
However, the developments presented above cannot be directly applied, since $Y_0 = 0$.
This is not useful in practice, since we are interested in a non-zero initial volatility model. Thus we need to modify the Hawkes processes sequence to obtain a non-degenerate initial volatility in the limit.
This feature can be achieved replacing μ_T by an inhomogeneous Poisson intensity $\hat{\mu}_T(t)$.

We recall the asymptotic framework of the previous section: consider sequence of probability spaces $(\Omega^T, \mathcal{F}^T, \mathbb{P}^T)$ on which $N^T = (N^{T,+}, N^{T,-})$ is a bi-dimensional Hawkes process defined on [0,T] and with intensity λ_t^T defined as (3.4.1). Since our goal is to design a sequence of processes leading in the limit to a rough Heston dynamic, we can consider specific assumptions on the matrix ϕ_T.
As described in [9], we use the heavy-tailed Mittag-Leffler function in order to define ϕ_T.

Assumption 7 *There exist $\beta \geq 0$, $1/2 < \alpha < 1$ and $\lambda > 0$ such that*

$$a_T = 1 - \lambda T^{-\alpha}\ ,\ \phi^T = \phi^T \chi$$

where

$$\chi = \frac{1}{\beta+1}\begin{pmatrix}1 & \beta\\ 1 & \beta\end{pmatrix} \ , \ \phi^T = a_T\phi \ , \ \phi = f^{\alpha,1}$$

with $f^{\alpha,1}$ the Mittag-Leffer density function.

This function is defined for $(\alpha,\gamma) \in (0,1)$ x $\mathbb{R}_+$ as

$$f^{\alpha,\gamma}(t) = \gamma t^{\alpha-1}E_{\alpha,\alpha}(-\gamma t^\alpha),\ t>0$$

where, given $(\alpha,\beta) \in (\mathbb{R}_+^*)^2, E_{\alpha,\beta}$ is the Mittag-Leffler function defined for $z \in \mathbb{C}$ as

$$E_{\alpha,\beta}(z) = \sum_{n\geq 0}\frac{z^n}{\Gamma(\alpha n+\beta)}$$

We recall we are working in the nearly unstable heavy tail case since

$$\int_0^\infty \phi(s)\,ds = 1$$

and

$$\alpha x^\alpha \int_x^\infty \phi(t)\,dt \to_{x\to\infty} \frac{\alpha}{\Gamma(1-\alpha)}$$

According to [9], we can state

Assumption 8 *The baseline intensity $\hat{\mu^T}$ is given by*

$$\hat{\mu^T} = \mu_T + \xi\mu_T\left(\frac{1}{1-a_T}\left(1-\int_0^t \phi^T(s)\,ds\right) - \int_0^t \phi^T(s)\,ds\right)$$

with $\xi > 0$ and $\mu = \mu T^{\alpha-1}$ for some $\mu > 0$.

We now state the behavior in the limit of our specific sequence of bi-dimensional nearly unstable Hawkes processes with heavy tails. For $t \in [0,1]$, we define

$$X_t^T = \frac{1-a_T}{T^\alpha\mu}N_{tT}^T \ , \ \Lambda_t^T = \frac{1-a_T}{T^\alpha\mu}\int_0^{tT}\lambda_s^T\,ds \ , \ Z_t^T = \sqrt{\frac{T^\alpha\mu}{1-a_T}}(X_t^T - \Lambda_t^T)$$

We obtain the following result:

Theorem 5 *As $T \to \infty$, the process $(\Lambda_t^T, X_t^T, Z_t^T)_{t\in[0,1]}$, under Assumptions 7 and 8, converges in law for the Skorokhod topology to Λ, X, Z where*

$$\Lambda_t = X_t = \int_0^t Y_s\, ds \begin{pmatrix} 1 \\ 1 \end{pmatrix} \ , \ Z_t = \int_0^t \sqrt{Y_s} \begin{pmatrix} dB_s^1 \\ dB_s^2 \end{pmatrix}$$

and Y is the unique solution of the rough stochastic differential equation

$$Y_t = \xi + \frac{1}{\Gamma(\alpha)} \int_0^t (t-s)^{\alpha-1} \lambda(1-V_s)\, ds + \lambda \sqrt{\frac{1+\beta^2}{\lambda\mu(1+\beta^2)}} \frac{1}{\Gamma(\alpha)} \int_0^t (t-s)^{\alpha-1} \sqrt{Y_s}\, dB_s$$

where

$$B = \frac{B^1 + \beta B^2}{\sqrt{1+\beta^2}}$$

and (B^1, B^2) is a bi-dimensional Brownian motion. Furthermore, for any $\epsilon > 0$, Y has Holder regularity $\alpha - 1/2 - \epsilon$.

Indeed, thanks to Theorem 5, we are now able to build the desired microscopic processes. For $\theta > 0$, let us define

$$P_t^T = \sqrt{\frac{\theta}{2}} \sqrt{\frac{1-a_T}{T^\alpha \mu}} (N_{tT}^{T,+} - N_{tT}^{T,-}) - \frac{\theta}{2} \frac{1-a_T}{T^\alpha \mu} N_{tT}^{T,+} = \sqrt{\frac{\theta}{2}} (Z^{T,+} - Z^{T,-}) - \frac{\theta}{2} X^{T,+} \tag{3.5.1}$$

We have the following corollary of Theorem 5.

Corollary 2 *As $T \to \infty$, under Assumptions 7 and 8, the sequence of processes $(P_t^T)_{t\in[0,1]}$ converges in law for the Skorokhod topology to*

$$P_t = \int_0^t \sqrt{V_s}\, dW_s - \frac{1}{2} \int_0^t V_s\, ds$$

where V is the unique solution of the rough stochastic differential equation

$$V_t = \theta\xi + \frac{1}{\Gamma(\alpha)} \int_0^t (t-s)^{\alpha-1} \lambda(\theta - V_s)\, ds + \lambda \sqrt{\frac{\theta(1+\beta^2)}{\lambda\mu(1+\beta^2)}} \frac{1}{\Gamma(\alpha)} \int_0^t (t-s)^{\alpha-1} \sqrt{V_s}\, dB_s$$

with (W, B) a correlated bi-dimensional Brownian motion which satisfies

$$d\langle W, B \rangle_t = \frac{1-\beta}{\sqrt{2(1+\beta^2)}} dt$$

So we have found a sequence of microscopic process as defined in (3.5.1) which converges to the rough Heston process.

3.6 Characteristic function of Rough Heston model

We set

$$V_0 = \xi\theta \ , \ \rho = \frac{1-\beta}{\sqrt{2(1+\beta^2)}} \ , \ \nu = \sqrt{\frac{\theta(1+\beta^2)}{\lambda\mu(1+\beta^2)}} \ , \ \lambda = \gamma$$

where λ and θ are the same as those in the dynamic of P^T. Remark that this implies that $\rho \in (-1/\sqrt{2}, 1/\sqrt{2}]$. We also write $P_t = \log(S_t/S_0)$.

We consider the rough Heston model:

$$\begin{aligned} dS_t &= S_t\sqrt{V_t}dW_t \\ V_t &= V_0 + \frac{1}{\Gamma(\alpha)}\int_0^t (t-s)^{\alpha-1}\gamma(\theta - V_s)\,ds + \frac{1}{\Gamma(\alpha)}\int_0^t (t-s)^{\alpha-1}\gamma\nu\sqrt{V_s}\,dB_s \end{aligned}$$

The parameters γ, θ, V_0 and ν are positive and play the same role as in the Heston model. W and B are two Brownian motions with correlation ρ.

The additional parameter α belongs to $(1/2, 1)$ and it governs the smoothness of the volatility sample paths. When $\alpha = 1$, we retrieve the classical Heston model. Therefore it is natural to view it as a rough version of Heston model and to call it rough Heston model. In the case $\alpha < 1$, the rough Heston model is not Markovian and the volatility process is no longer a semi-martingale.

Our main result is that, quite surprisingly, the characteristic function of the log-price in rough Heston models exhibits the same structure as the one obtained in the classical Heston model. The difference is that the Riccati equation is replaced by a fractional Riccati equation, where a fractional derivative appears instead of a classical derivative. More precisely, we obtain

Theorem 6 *Consider the rough Heston model with a correlation between the two Brownian motions ρ satisfying $\rho \in (-1/\sqrt{2}, 1/\sqrt{2}]$. For all $t \geq 0$, we have*

$$L(a,t) = \exp\left(g_1(a,t) + V_0 g_2(a,t)\right)$$

where

$$g_1(a,t) = \theta\gamma\int_0^t h(a,s)\,ds \ , \ g_2(a,t) = I^{1-\alpha}h(a,t)$$

and $h(a,\cdot)$ is solution of the following fractional Riccati equation:

$$D^{\alpha}h(a,t) = \frac{1}{2}(-a^2 - ia) + \gamma(ia\rho\nu - 1)h(a,s) + \frac{(\gamma\nu)^2}{2}h^2(a,s) \ , \ I^{1-\alpha}h(a,0) = 0$$

with D^{α} and $I^{1-\alpha}$ the fractional derivative and integral operators.

Remark that when $\alpha = 1$, this result coincides with the classical Heston result. However, note that for $\alpha < 1$, the solutions of such Riccati equations are no longer explicit.

We define the fractional integral of order $r \in (0,1]$ of a function f as

$$I^r f(t) = \frac{1}{\Gamma(r)} \int_0^t (t-s)^{r-1} f(s)\, ds$$

and the fractional derivative of order $r \in [0,1)$ as

$$D^r f(t) = \frac{1}{\Gamma(1-r)} \frac{d}{dt} \int_0^t (t-s)^{-r} f(s)\, ds$$

whenever they exist.

Thus we have been able to obtain a semi-closed formula for the characteristic function in rough Heston models.
The difference between the classical case and the rough one is essentially the fact that, in the Riccati equation, the classical derivative is replaced by a fractional derivative. The drawback is that such fractional Riccati equation does not have explicit solutions.
However, they can be solved numerically, as we will see in the following chapters.

Chapter 4

Fourier method for option pricing

4.1 Introduction

In the first years of this century, the Fourier transform techniques have played an important role in the derivative pricing world.
Fourier inversion methods allow us to price different types of derivatives contracts in the case we know analitically or numerically the characteristic function of the underlying stochastic price process.
This is the reason why we use these techniques when dealing with Heston model.
In this section, we will explain both the theoretical framework and the practical approach of the Fourier transform in the financial world (see [7]).

In particular, in our codes, all the computation are explicit (see Appendix A) and we don't use the Fast Fourier transform.
All the formulas listed below produce reasonable result but, when we implement the code, we decide to follow the Lewis' one. This is a widely adopted formula because of its simplicity.

4.2 Fourier transform and Inversion Theorem

Directly modelling the option payoff with an analytical stochastic process is not an easy task.
Usually the option values are computed by mapping the characteristic function of the density of these processes to the payoff in the Fourier space. This idea gives rise to the inversion methods.

These procedures allow us to take an integral of the payoff function over the probability distribution obtained by inverting the corresponding Fourier transform. Calculation in Fourier space are usually less complex than the ones in spatial domains. The solution of the problem in the Image space is described through an Image function and, finally, to obtain the solution in the original space, we need to invert the Fourier function with the inversion method.
Transform tools become very effective when we deal with complex models which are more simply specified through a characteristic function rather than a probability distribution.

The inversion method was first proposed by Stein and Stein (1991) in order to find the underlying distribution in stochastic volatility model. Then Heston in 1993 found an analytical formula for European option valuation where the volatility of the underlying was a function of time.
Starting from these two works, Bankshi and Madan (2000) developed a general pricing formula using the characteristic function.
Carr and Madan in 1999 introduced a numerical method based on the fast Fourier Transform, mapping the Fourier transform directly to call option prices via the price process characteristic function.
Following them, Lewis and others developed pricing algorithm based on Fourier transformed payoff function. We will list them in the next sections.

The power of Fourier transform methods is linked with the fact that it is always possible to obtain the characteristic function of a random variable, while we cannot state the same about the analytical expression.
If we know (analytically o numerically) the characteristic function, we can compute the distribution function via Inversion theorem. There is a bijective relation between characteristic function and distribution function and this is the message state by the theorem mentioned above. The link between the

two faces of the medal is an inverse Fourier transform.

Following [7], we state two formulas based on the Gil-Peleaz inversion integral, which shows the reciprocal link between the characteristic function $\phi_X(u)$ and the probability density function $f_X(x)$ of a real valued random variable X:

$$\phi_X(u) = \mathbb{E}[e^{iuX}] = \int_{-\infty}^{\infty} e^{iux} f_X(x) dx$$

$$f_X(x) = \mathbb{F}^{-1}[\phi_X(u)] = \frac{1}{2\pi} \int_{-\infty}^{\infty} e^{-iux} \phi_X(u) du$$

where $\mathbb{F}[\cdot]$ denotes the Fourier transform.

4.3 Pricing Formulas using Characteristic function

In literature, there are two classes of invertion methods.
The first approach provides a Black-Scholes like formula for option prices inverting the cumulatuve distribution function $F_X(x) = \mathbb{P}(X \leq x) = \int_{-\infty}^{x} f_X(x)dx$.
The most remarkable result based on this idea is obtained by Bakshi and Madan.
The second class is composed by the methods which invert the probability density function. Carr and Madan related the characteristic function to the Fourier transform of an option. Also Lewis exploited the same idea, but the domain of integration is different between the two models. This happens in order to ensure the trasformation existence.
Both the approaches are applicable to a wide range of European options.

Consider the problem of valuing a European call of maturity T, written on the spot price at maturity S_T of some underlying asset. The characteristic function of $x_T = \log(S_t)$ is defined by

$$\phi(u; t, T, x, v) = \mathbb{E}\left[\exp(iux_T) \mid x_t = x, V_t = v\right]$$

Assume that the characteristic function is known analytically.

4.3.1 The Black–Scholes Style Formula - Bakshi and Madan (2000)

Assuming no dividends and constant interest rates r, the initial option value can be determined as

$$C(S_0, K, T) = S_0\Pi_1 - Ke^{-rT}\Pi_2$$

where

$$\Pi_1 = \frac{1}{2} + \frac{1}{\pi}\int_0^\infty Re\left(\frac{e^{-iu\log(K)}\phi_T(u-i)}{iu\phi_T(-i)}\right)du$$
$$\Pi_2 = \frac{1}{2} + \frac{1}{\pi}\int_0^\infty Re\left(\frac{e^{-iu\log(K)}\phi_T(u)}{iu}\right)du$$

Moreover, the two integrals Π_1 and Π_2 can be combined into one integral. By rearranging the involved equations the Black and Scholes style formula for a call option reduces to

$$\begin{aligned} C(S_0, K, T) = {} & \frac{1}{2}(S_t - e^{-rT}K) + \\ & + \frac{1}{\pi}\int_0^\infty \Big[S_0 Re\left(\frac{e^{iu\log(K)}\phi_T(u-i)}{iu}\right) + \\ & - e^{-rT}KRe\left(\frac{e^{iu\log(K)}\phi_T(u)}{iu}\right)\Big]du \end{aligned}$$

4.3.2 Attari's approach (2004)

Attari was able to obtain a formula involving a single one dimensional intergral.
Starting from a Black-Scholes style solution,

$$C(S_0, K, T) = S_0\Pi_1 - Ke^{-rT}\Pi_2$$

where

$$\Pi_1 = 1 + \frac{e^{\log K}}{2\pi}\int_{-\infty}^{\infty}\frac{e^{-iu\log(K)}\phi_T(u)}{i(u+i)}\,du$$
$$\Pi_2 = \frac{1}{2} + \frac{1}{2\pi}\int_{-\infty}^{\infty}\frac{e^{-iu\log(K)}\phi_T(u)}{iu}\,du$$

the call value can be obtained

$$C(S_0,K,T) = S_0\left(1+\frac{e^{\log K}}{2\pi}\int_{-\infty}^{\infty}\frac{e^{-iu\log(K)}\phi_T(u)}{i(u+i)}\,du\right)+$$
$$-e^{-rT}K\left(\frac{1}{2}+\frac{1}{2\pi}\int_{-\infty}^{\infty}\frac{e^{-iu\log(K)}\phi_T(u)}{iu}\,du\right)$$

Rearranging the terms and exploiting Euler identity and symmetry for real valued function,

$$C(S_0,K,T) = \frac{1}{2}(S_t - e^{-rT}K)+$$
$$+e^{-rT}K\frac{1}{\pi}\int_0^{\infty}\left[\frac{\left(Re[\phi(u)]+\frac{Im[\phi(u)]}{u}\right)cos(u\ log(K))}{1+u^2}+\right.$$
$$\left.+\frac{\left(Im[\phi(u)]-\frac{Re[\phi(u)]}{u}\right)sin(u\ log(K))}{1+u^2}\right]du$$

which is a single one dimensional integration formula. The quadratic term at denominator ensures a faster convergence.

4.3.3 Bates' approach (2006)

As the previous result, this formulation requires only one integration and the integrand converge faster than the Black-Scholes type solution, due to the quadratic term in the denominator.

$$C(S_0,T,K) = S_0 - e^{-rT}K\left(\frac{1}{2}+\frac{1}{2\pi}\int_{-\infty}^{\infty}\frac{e^{-iu\log(\frac{K}{S_0})}\phi_T(u)}{iu(1-iu)}\,du\right)$$
$$= S_0 - e^{-rT}K\left(\frac{1}{2}+\frac{1}{\pi}\int_0^{\infty}Re\left(\frac{e^{-iu\log(\frac{K}{S_0})}\phi_T(u)}{iu(1-iu)}\right)\,du\right)$$

where S_0 is an integration constant (value of a zero-strike call).

4.3.4 Carr and Madan approach (1999)

Carr and Madan developed a different approach based on the fast Fourier transform (FFT). Unfortunately, the FFT cannot be applied to evaluate the previous integrals, since the integrands are singular at the evaluation point $u = 0$.
The new idea consists in calculating the Fourier transform of a modified call option price with respect to the logarithmic strike price k. The advantage of the FFT is explained by the name itself: if allows to price an high number of options within a single Fourier inversion.
Defined

$$C_T(k) = e^{-rT}\mathbb{E}^{\mathbb{Q}}[(S_T - K)^+]$$

where $\mathbb{Q}$ is the martingale measure, $C(k)$ is not L^1 and a Fourier transform does not exist. Nevertheless, introducing an exponential damping factor $e^{\alpha k}$ with $\alpha > 0$ allows us to define

$$c_T(k) = e^{\alpha k} C_T(k)$$

where the modified call price $c_T(k)$ is an integrable function, since

$$\int_{-\infty}^{\infty} \left| e^{\alpha k} C_T(k) \right| \, dk < \infty$$

The Fourier transform of $c(k)$ is given by

$$\psi(u) = \int_{-\infty}^{\infty} e^{iuk} c(k) \, dk = \frac{e^{-rT}\phi_T(u - (\alpha + 1)i)}{\alpha^2 + \alpha - u^2 + i(2\alpha + 1)u}$$

where $\psi(u)$ is expressed in terms of the characteristic function ϕ_T. A complete proof of this last formula is present in [7].
Given $\psi(u)$, an inverse Fourier transform multiplied by the reciprocal of the exponential factor yields to the undamped call prices

$$\begin{aligned} C_T(k) &= \frac{e^{-\alpha k}}{2\pi} \int_{-\infty}^{\infty} e^{-iuk} \psi(u) \, du \\ &= \frac{e^{-\alpha k}}{\pi} \int_{0}^{\infty} Re\left(e^{-iuk} \psi(u) \right) \, du \end{aligned} \tag{4.3.1}$$

We can use this method when α allows a good computational behaviour. A sufficient condition for the integrability of $c_T(k)$ is given by $\psi(0)$ being finite.

The Carr and Madan approach is different from other models because not only the density function, but the whole option price is Fourier transformed. The most relevant difference stays in the formula (4.3.1) which practically is a generalized Fourier transform:

$$\begin{aligned}\frac{1}{2\pi}\int_{iz_i-\infty}^{iz_i+\infty} e^{-izk}\psi(z)dz_r &= \frac{1}{\pi}\int_{iz_i+\infty}^{iz_i} Re[e^{-izk}\psi(z)]dz_r \\ &= \frac{e^{z_i k}}{\pi}\int_0^{\infty} Re[e^{-z_r k}\psi(z_r+iz_i)]dz_r\end{aligned}$$

This feature removes the pole in the origin and shifts it in the imaginary axis. This leads to a less sensitive numerical evaluation.

4.3.5 Lewis' approach (2001)

Lewis followed the Carr-Madan route.
The core of his work is the idea to express the option value as convolution of generalized Fourier transforms. The transform representations of option prices can be seen as contour integrals in the complex plane. By shifting the contours, Lewis generated a new pricing formula.

Each derivative has its own payoff function $w(S_T)$. Carr and Madan transformed the whole option price including the payoff function, while Lewis represented also the payoff functions in Fourier space

$$\hat{w}(z) = \int_{-\infty}^{\infty} e^{izx} w(x)\, dx$$

The problem is that $(e^x - K)^+$ is not a L^1 function and the Fourier transform does not exist.

Like in Carr-Madan approach, Lewis introduced an exponential damping factor. For the modified payoff, we obtain the regular Fourier transform, since $(e^x - K)^+ e^{-z_i x} \to 0$ as $x \to \infty$ for some appropriate z_i. This corresponds to a Fourier transform along a line in the complex plane where the path of integration is parallel to the real axis. The calculation (see [7]) for the call option payoff yields to

$$\hat{w}(z) = -\frac{K^{iz+1}}{z^2 - iz}$$

with z being a complex valued number. The upper limit $x = \infty$ only exists under the condition $Im[z] > 1$ which implies that the Fourier transform well behaves only within a certain strip of regularity $\mathcal{S}_w$ in the complex plain.

Given the generalized payoff transform, the corresponding inverse transformation is

$$w(x) = \frac{1}{2\pi} \int_{iz_i-\infty}^{iz_i+\infty} e^{-izx} \hat{w}(z)\, dz$$

Assuming that we have a well defined characteristic function $\phi_T(u)$ for an arbitrary price dynamics and a transformed payoff $\hat{w}(z)$ with $z \in \mathcal{S}_w$, we can obtain the option value

$$\begin{aligned} V(S_0, K, T) &= e^{-rT} \mathbb{E}^{\mathbb{Q}} \left[w(x) \right] \\ &= \frac{e^{-rT}}{2\pi} \mathbb{E}^{\mathbb{Q}} \left[\int_{iz_i-\infty}^{iz_i+\infty} e^{-izx} \hat{w}(z)\, dz \right] \\ &= \frac{e^{-rT}}{2\pi} \int_{iz_i-\infty}^{iz_i+\infty} \mathbb{E}^{\mathbb{Q}} \left[e^{-izx} \right] \hat{w}(z)\, dz \\ &= \frac{e^{-rT}}{2\pi} \int_{iz_i-\infty}^{iz_i+\infty} \phi_T(-z) \hat{w}(z)\, dz \end{aligned}$$

Applying the payoff transform of a call option, the call price is given by

$$C(S_0, K, T) = S_0 - \frac{K e^{-rT}}{2\pi} \int_{iz_i+\infty}^{iz_i-\infty} e^{-izk} \phi_T(-z)\, \frac{dz}{z^2 - iz}$$

with $k = \log \frac{S_0}{K} + rT$ in the phase factor e^{-izk} and $z_i \in \mathcal{S}_v$.
By moving the integration contour to $z_i \in (0, 1)$ and choosing $z_i = \frac{1}{2}$, we obtain a simmetric path of integration. Finally, we can change the variable $z = u + \frac{i}{2}$ and obtain these alternative formulas:

$$\begin{aligned} C(S_0, K, T) &= S_0 - \frac{\sqrt{SK} e^{\frac{-rT}{2}}}{\pi} \int_0^{\infty} Re \left[e^{-iuk} \phi_T(-u - \frac{i}{2}) \right] \frac{du}{u^2 + \frac{1}{4}} \\ &= S_0 - \frac{\sqrt{SK} e^{\frac{-rT}{2}}}{\pi} \int_0^{\infty} Re \left[e^{iuk} \phi_T(u - \frac{i}{2}) \right] \frac{du}{u^2 + \frac{1}{4}} \end{aligned}$$

In particular, in our implementation, we will evaluate the price with this last formula (see Appendix A).

Chapter 5

Numerical analysis of convolution equations

5.1 Introduction

In rough volatility models, due to the non-Markovian nature of the fractional driver, partial differential equations can no longer be used and simulation is the only available route.
Despite the availability of efficient Monte Carlo schemes, pricing and model calibration in rough volatility models remain time-consuming.
We focus on the description of the short-time behavior of the at-the-money implied volatility skew of the stochastic volatility process. Fukusawa in [2] established that the blow-up in this slope (observed in real market data) can be described by a volatility process σ such that ATM volatility skew has the form $\psi(\tau) \sim \tau^{H-1/2}$, at least for small τ. This property is satisfied by stochastic volatility models based on the fractional Brownian motion with Hurst parameter $H < \frac{1}{2}$.

5.2 The Predictor-Corrector approach

In our computation, we follow the general pseudo code of the classical one step Adams-Bashforth-Moulton algorithm for first-order equations presented in [1].
In this section, we will explain the general setting where the results provided in [1] holds true.

A fractional differential equation can be defined as

$$\begin{cases} D^{\alpha}y(x) = f(x, y(x)) \\ y^{(k)}(0) = y_0^{(k)},\ k = 0, 1...m-1 \end{cases} \tag{5.2.1}$$

where $m := \lceil \alpha \rceil$ is just the value α rounded up to the nearest integer.
This initial value problem is equivalent to the Volterra integral equation

$$y(x) = \sum_{k=0}^{\lceil \alpha \rceil - 1} y_0^{(k)} \frac{x^k}{k!} + \frac{1}{\Gamma(\alpha)} \int_0^x (x-t)^{\alpha-1} f(t, y) dt \tag{5.2.2}$$

in the sense that a continuos function is a solution of the initial value problem if and only if is a solution of (5.2.2).

This is the exact framework where we will work: we need a method to approximate a solution of the Volterra integral equation derived from the Heston model.

However, a large number of steps and computational time are required to achieve satisfactory accuracy. We choose a scheme with 1000 steps.

5.3 Numerical scheme

In the following section, we show how to compute numerically the log-price characteristic function in the rough Heston model.
Starting from the Theorem 6, $L_p(a,t)$ can be described through the fractional Riccati equation

$$D^\alpha h(a,t) = F(a,h(a,t)) \ , \ I^{1-\alpha}h(a,0) = 0$$

where

$$F(a,x) = \frac{1}{2}(-a^2 - ia) + \gamma(ia\rho\nu - 1)x + \frac{(\gamma\nu)^2}{2}x^2 \tag{5.3.1}$$

These equations imply the following Volterra equation:

$$h(a,t) = \frac{1}{\Gamma(\alpha)}\int_0^t (t-s)^{\alpha-1}F(a,h(a,s))ds$$

which enjoys the property mentioned in the section above and so we can follow the pseudo-algorithm described in [1].
The necessary specification in order to use it are listed below.

We write $g(a,t) = F(a,h(a,t))$. Over a regular time grid $(t_k)_{k\in\mathbb{R}}$ with mesh $\Delta(t_k = k\Delta)$, we estimate

$$h(a,t_{k+1}) = \frac{1}{\Gamma(\alpha)}\int_0^{t_{k+1}} (t_{k+1}-s)^{\alpha-1}g(a,s)ds$$

with

$$\frac{1}{\Gamma(\alpha)}\int_0^{t_{k+1}} (t_{k+1}-s)^{\alpha-1}\hat{g}(a,s)ds$$

where

$$\hat{g}(a,t) = \frac{t_{j+1}-t}{t_{j+1}-t_j}\hat{g}(a,t_j) + \frac{t-t_j}{t_{j+1}-t_j}\hat{g}(a,t_{j+1}),\ t\in[t_j,t_{j+1}),\ 0\le j\le k$$

This is a trapezoidal discretization of the fractional integral and we are led to the scheme:

$$\hat{h}(a,t_{k+1}) = \sum_{0\le j\le k} a_{j,k+1}F(a,\hat{h}(a,t_j)) + a_{k+1,k+1}F(a,\hat{h}(a,t_{k+1})) \tag{5.3.2}$$

with

$$a_{0,k+1} = \frac{\Delta^\alpha}{\Gamma(\alpha+2)}(k^{\alpha+1} - (k-\alpha)(k+1)^\alpha)$$

$$a_{j,k+1} = \frac{\Delta^\alpha}{\Gamma(\alpha+2)}((k-j+2)^{\alpha+1} - 2(k-j+1)^{\alpha+1}),\ 1 \leq j \leq k$$

$$a_{k+1,k+1} = \frac{\Delta^\alpha}{\Gamma(\alpha+2)}$$

Being $\hat{h}(a, t_{k+1})$ on the right and on the left of (5.3.2), the scheme is implicit. In a first step, we need to compute a pre-estimation of $\hat{h}(a, t_{k+1})$ in order to plug it in the trapezoidal formula. This predictor is denoted by $\hat{h}^P(a, t_{k+1})$ and defined as:

$$\hat{h}^P(a, t_{k+1}) = \frac{1}{\Gamma(\alpha)} \int_0^t (t-s)^{\alpha-1} \tilde{g}(a, s) ds$$

with

$$\tilde{g}(a, t) = \hat{g}(a, t_j),\ t \in [t_j, t_{j+1}),\ 0 \leq j \leq k$$

So,

$$\hat{h}^P(a, t_{k+1}) = \sum_{0 \leq j \leq k} b_{j,k+1} F(a, \hat{h}(a, t_j))$$

where

$$b_{j,k+1} = \frac{\Delta^\alpha}{\Gamma(\alpha+1)}((k-j+1)^\alpha - (k-j)^\alpha),\ 0 \leq j \leq k$$

The final explicit numerical scheme is:

$$\hat{h}(a, t_{k+1}) = \sum_{0 \leq j \leq k} a_{j,k+1} F(a, \hat{h}(a, t_j)) + a_{k+1,k+1} F(a, \hat{h}^P(a, t_{k+1})),\ \hat{h}(a, 0) = 0$$

where the weights $a_{j,k+1}$ are given by (5.3).

In particular, we can guarantee from [9] that for a given $t > 0$ and $a \in \mathbb{R}$,

$$max_{t_j \in [0,t]} |\hat{h}(a, t_j) - h(a, t_j)| = o(\Delta)$$

and

$$max_{t_j \in [\epsilon,t]} |\hat{h}(a, t_j) - h(a, t_j)| = o(\Delta^{2-\alpha})$$

for any $\epsilon > 0$.

5.4 The Predictor-Corrector algorithm

In order to reproduce the exact framework we talk about in the section 5.2, we recall from (5.3.1) that F is a function of two variables. So in our algorithm we fix the variable a and we consider F as a variable of $h(t)$.
Since we don't have the derivative in time, the pseudo algorithm presented in [1] can be simplified.

Here we propose the version that we have used in our computation.

α in (5.2.1) represents the order of the derivative, but, since we are dealing with a fractional derivative, $\lceil \alpha \rceil$ is equal to one. So in (5.2.2), we can ignore the summation.

Considering the inputs:

- f: the function which define the right side of the differential equation (the F defined in (5.3.1))
- T: time to expiry
- N: number of time steps

we can state this pseudo-algorithm:

1. h:=T/N
2. for k=1 to N
   $b(k) := k^{\alpha} - (k-1)^{\alpha}$
   $a(k) := (k+1)^{\alpha+1} - 2k^{\alpha+1} + (k-1)^{\alpha+1}$
   end
3. $y(0) = y_0$

4. for j=1 to N

$$p = \frac{h^\alpha}{\Gamma(\alpha+1)} \sum_{k=0}^{j-1} b(j-k) f(kh, y(k))$$

$$y(j) = \frac{h^\alpha}{\Gamma(\alpha+2)} \big(f(jh, p) + ((j-1)^{\alpha+1} - (j-1-\alpha) j^\alpha) f(0, y(0)) + \sum_{k=1}^{j-1} a(j-k) f(kh, y(k)) \big)$$

end

The output y contains the approximate solution in each point of the time grid (so the $\hat{h}$ in the section 5.3).
This is only a general representation of the Adams scheme. One can find the exact implementation of the algorithm for the rough Heston model in the Appendix A.2.

5.5 Numerical illustration

Considering the following parameters:

$$\nu = 0.05,\ \gamma = 2,\ \rho = -0.5,\ \theta = 0.04,\ V_0 = 0.04,\ \alpha = 0.62$$

we compare in figure 5.1 the ATM skew produced by the classical Heston model and its rough counterpart. We highligt that the rough Heston model is able to reproduce the exploding structure of the skew when the time to maturity goes to zero.

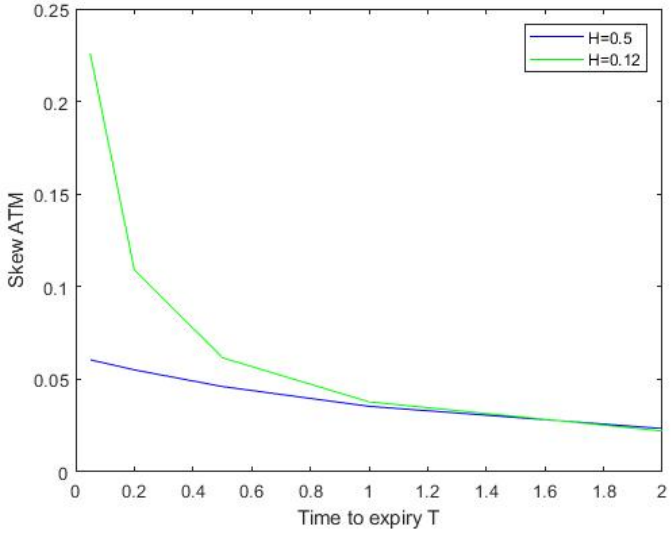

Figure 5.1: ATM skew as a function of maturity

Chapter 6

Multifactor Approximation

6.1 Introduction

Rough volatility models are very appealing because they fit both historical and implied volatility. However, they are not longer Markovian and there is not a simple way to simulate efficiently these models. So derivatives pricing and hedging are a problematic task.
The introduction of the fractional kernel implies the loss of the Markovian property and the semi-martingale structure of the volatility process.
Following [6] and [3], we approximate the rough Heston model with a simpler one that we can use in practice. We aim to design a "multi-factor" stochastic model which enjoys the Markov property.

Recalling the rough Heston model

$$dS_t = S_t\sqrt{V_t}dW_t$$
$$V_t = V_0 + \frac{1}{\Gamma(\alpha)}\int_0^t (t-s)^{\alpha-1}\gamma(\theta - V_s)\,ds + \frac{1}{\Gamma(\alpha)}\int_0^t (t-s)^{\alpha-1}\nu\sqrt{V_s}\,dB_s$$

and the equivalence between α and the Hurst index

$$H = \alpha + \frac{1}{2},$$

the basic idea is to approximate the fractional kernel $K(t) = \frac{t^{H-1/2}}{\Gamma(H+1/2)}$ as a Laplace transform of a positive measure μ

$$K(t) = \int_0^\infty e^{-\beta t}\mu(d\beta);\;\; \mu(d\beta) = \frac{\beta^{-H-1/2}}{\Gamma(H+1/2)\Gamma(1/2-H)}d\beta$$

Then we approximate μ by a finite sum of Dirac measures $\mu^n = \sum_{i=1}^n c_i^n \delta_{\beta_i^n}$ with positive weights $(c_i^n)_{1\leq i\leq n}$ and mean reversion $(\beta_i^n)_{1\leq i\leq n}$, for $n \geq 1$.
Finally, we obtain a sequence of smoothed kernels $(K^n)_{n\geq 1}$ given by

$$K^n(t) = \sum_{i=1}^n c_i^n e^{-\beta_i^n t}, \;\; n \geq 1$$

This approximation allows us to define the multi-factor Heston model $(S^n, V^n) = (S_t^n, V_t^n)_{t\leq T}$:

$$\begin{aligned} dS_t^n &= S_t^n \sqrt{V_t^n} dW_t \\ V_t^n &= g_n(t) + \sum_{1=1}^n c_i^n V_t^{n,i} \end{aligned} \tag{6.1.1}$$

where

$$\begin{aligned} dV_t^{n,i} &= (-\beta_i^n V_t^{n,i} - \gamma V_t^n)dt + \nu\sqrt{V_t^n} dB_t \\ g^n(t) &= V_0 + \theta \int_0^t K^n(t-s)ds \end{aligned}$$

endowed with the initial conditions

$$S_0^n = S_0, \;\; V_0^{n,i} = 0$$

The model is Markovian with respect to the spot price and n variance factors $(V^{n,i})_{1\leq i\leq n}$.

The factors share the same dynamics, but they mean revert at different speed $(\beta_i^n)_{1\leq i\leq n}$.
In [6], the authors assure the strong existence and uniqueness of the model (S^n, V^n). In particular, they guarantee that the multi-factor approximation converges to the rough volatility model, when the number of factors goes to infinity and the coefficients $(c_i^n, \beta_i^n)_{1\leq i\leq n}$ are chosen in a suitable way.

In particular, in the previous chapters, we derive the characteristic function of the log-price in the rough Heston model as a solution of a fractional Riccati equation.
The multifactor approximation inherits an affine structure: the fractional Riccati equation can be substitued for a n-dimensional classical Riccati equation. So, considering a large n, we can solve numerically n ordinary Riccati equation instead of computing the solution with the Adams scheme.

6.2 The multi-factor scheme for the fractional Riccati equation

Consider the model defined in (6.1.1).
The dynamics of (S^n, V^n) in terms of Volterra equation with the smoothed kenel K^n is:

$$dS_t^n = S_t^n \sqrt{V_t^n} dW_t$$
$$V_t^n = g_n(t) - \int_0^t K^n(t-s)\gamma V_s^n ds + \int_0^t K^n(t-s)\nu\sqrt{V_s^n} dB_s$$

We slightly modify the characteristic function formula and we state that

$$L^n(t,a) = \mathbb{E}\left[e^{iaX_t}\right]$$

is given by

$$exp\left(\int_0^t F(a, \psi^n(t-s,a))g^n(s)ds\right)$$

where $\psi^n(\cdot, a)$ is the unique solution of the Riccati equation

$$\psi^n(t,a) = \int_0^t K^n(t-s)F(a,\psi(s,a))ds,\ t \in [0,T]$$

and

$$F(a,x) = \frac{1}{2}(-a^2 - a) + (u\rho\nu - \gamma)x + \frac{\nu^2}{2}x^2$$

for a $\in \mathbb{C}$, with $Re(u) \in [0,1]$.

As established in [6], $(S^n, V^n)_{n\geq 1}$ converges in law to the rough Heston model (S, V) when n tends to infinity.
Moreover, the pointwise convergence of $L^n(t,a)$ to the original characteristic function implies that $\psi^n(\cdot, a)$ is close to the solution of the fractional Riccati equation.

Because of this, in [6], the authors suggest a new numerical method aimed to compute the fractional Riccati solution. Given that

$$\psi^{n,i}(t,a) = \int_0^t e^{-\beta_i^n(t-s)}F(a,\psi^n(s,a))ds, \quad i \in \{1,...,n\}$$

define

$$\psi^n(t,a) = \sum_{i=1}^{n} c_i^n \psi^{n,i}(t,a).$$

$(\psi^{n,i}(\cdot,a))_{1\ leqi\leq n}$ solves the n-dimensional system of ordinary Riccati equation

$$\begin{cases} \partial_t \psi^{n,i}(t,a) = -\beta_i^n \psi^{n,i}(t,a) + F(a,\psi(t,a)) \\ \psi^{n,i}(0,a) = 0, \quad i \in \{1,...,n\} \end{cases}$$

We can solve the system with standard finite difference method and, at the end, we obtain $\psi^n(\cdot,a)$ that is the approximation of the fractional Riccati solution.

6.3 The lifted Heston model

Following [3], in this section we introduce the lifted Heston model, a specification of the multi-factor approximation for stochastic volatility models.
As said above, the approximated variance process is built as a weighted sum of n factors driven by the same one-dimensonal Brownian motion.

If we consider the two extreme cases in the multi-factor model, we recover the classical Heston if $n = 1$ and its rough counterpart when n goes to infinity. The lifted model enjoys the best of the two worlds: it can reproduce the ATM skew as a rough volatility model and it is Markovian like the classical Heston. So, we can obtain the log-price characteristic function solving a finite system of ordinary Riccati differential equations.
The lifted model can be more easily implemented than the rough one, but it still remains precise about the implied volatility.

Recalling the multi-factor model (6.1.1), we stress that all the factors $(V^{n,i})_{1\leq i\leq n}$ start from zero and share the same one-dimensional Brownian motion W, but the mean-reverting speed $(\beta_i^n)_{1\leq i\leq n}$ is different for each volatility factor.

Since we need to compare the lifted model to the other considered in this work, we focus on the structure of g_n. This function allows us to plug in the initial term-structure in the model.
As suggested in [3], we will consider only a certain type of g_n, in particular

the form:

$$g_0^n(t) = V_0 + \gamma\theta \sum_{i=1}^{n} c_i^n \int_0^t e^{-\beta_i^n (t-s)} ds \tag{6.3.1}$$

where V_0 and θ are non-negative parameters.

Setting $n = 1$, $c_1^1 = 1$ and $\beta_1^1 = 0$, the lifted Heston model degenerates into the classical one. In the Appendix A.4, we provide a function to compare the two models. In particular, we obtain that the Mean Squared Error between the two models prices is in the order of 1e-05.

At first glance, the model seems over-parametrized since we need to consider all the coefficients $(c_i^n, \beta_i^n)_{1 \le i \le n}$. So, the lifted model has the same five parameters $(V_0, \theta, \gamma, \nu, \rho)$ of the Heston model plus $2n$ additional parameters for weights and mean reversion.
However, we can provide a good parametrization of these $2n$ factors in terms of two coefficients, the Hurst index and the artificial parameter r_n. In this way, we are able to reduce our problem dimension.
So, we start with $(2n+5)$ parameters and we end up with only 7 coefficients $(V_0, \theta, \gamma, \nu, \rho, H, r_n)$. This result is remarkable especially when dealing with the model calibration.

For a fixed even number of factors n, we fix $r_n > 1$ and we consider the following parametrization for weights and mean reversion coefficients:

$$\begin{aligned} c_i^n &= \frac{(r_n^{1-\alpha} - 1) r_n^{(\alpha-1)(1+n/2)}}{\Gamma(\alpha)\Gamma(2-\alpha)} r_n^{(1-\alpha)i} \\ \beta_i^n &= \frac{1-\alpha}{2-\alpha} \frac{r_n^{2-\alpha} - 1}{r_n^{1-\alpha} - 1} r_n^{i-1-n/2} \end{aligned} \tag{6.3.2}$$

where $i = 1, ..., n$ and $\alpha := H + 1/2$ for some $H \in (0, 1/2)$.
Moreover, if the sequence $(r_n)_{n \ge 1}$ satisfies

$$r_n \downarrow 1 \text{ and } \; n \cdot ln(r_n) \to \infty \text{ as } \; n \to \infty, \tag{6.3.3}$$

it can be proven the convergence of the lifted Heston model towards the rough one (for the proof, see [3]).

Here we state the convergence theorem towards the rough Heston.

Theorem 7 *Consider a sequence $(r_n)_{n\geq 1}$ satistisfying (6.3.3), set g_n as in (6.3.1) and $(c_i^n, \beta_i^n)_{1\leq i\leq n}$ as in (6.3.2), for every even n=2p, with $p \geq 1$. Assume $S_0^n = S_0$ for all n, then the sequence of solutions $(S^n, V^n)_{n=2p,p\geq 1}$ defined as (6.1.1) converges weakly on the space of continuous functions on [0,T] endowed with the uniform topology, towards the rough Heston model for any $T > 0$.*

6.4 Numerical analysis

6.4.1 Numerical scheme

In our computation, we follow the approximation scheme for the n-dimensional Riccati equations system given in the appendix of [3].

We consider an explicit-implicit discretization scheme as follows:

$$\begin{cases} \psi_{t_{k+1}}^{n,i} = \dfrac{1}{1+\beta_i^n \Delta t}\Big(\psi_{t_k}^{n,i} + \ F\Big(a, \sum_{j=1}^n c_j^n \psi_{t_k}^{n,j}\Big)\Big) \\ \psi_0^{n,i} = 0, \ \ i = 1, ..., n \end{cases}$$

for a regular time grid $t_k = k\Delta t$ for all $k = 1, ..., N$, where T is the terminal time, N is the number of time steps and $\Delta t = T/N$.

6.4.2 Quality of the approximation

For each $n \in \{10, 20, 50\}$, we generate the implied volatility surface with the Lifted Heston considering n factors. We observe the convergence of the approximation to the rough result.

Considering the following parameters:

$$\nu = 0.3, \ \gamma = 0.3, \ \rho = -0.7, \ \theta = 0.02, \ V_0 = 0.02, \ \alpha = 0.6$$

we obtain figure 6.1 and 6.2 that represent how well we can approximate the rough model with the multifactor approach. We consider two distinct time to maturity, T=1 week and T=1 year.
In both cases, we can see some numerical instabilities in the right part of the figures. This happens because our numerical scheme is not accurate if the

Call option is out of the money. In order to satisfy the condition (6.3.3), we define the following sequence

$$r_n = 1 + 10n^{-0.9}, n \geq 1$$

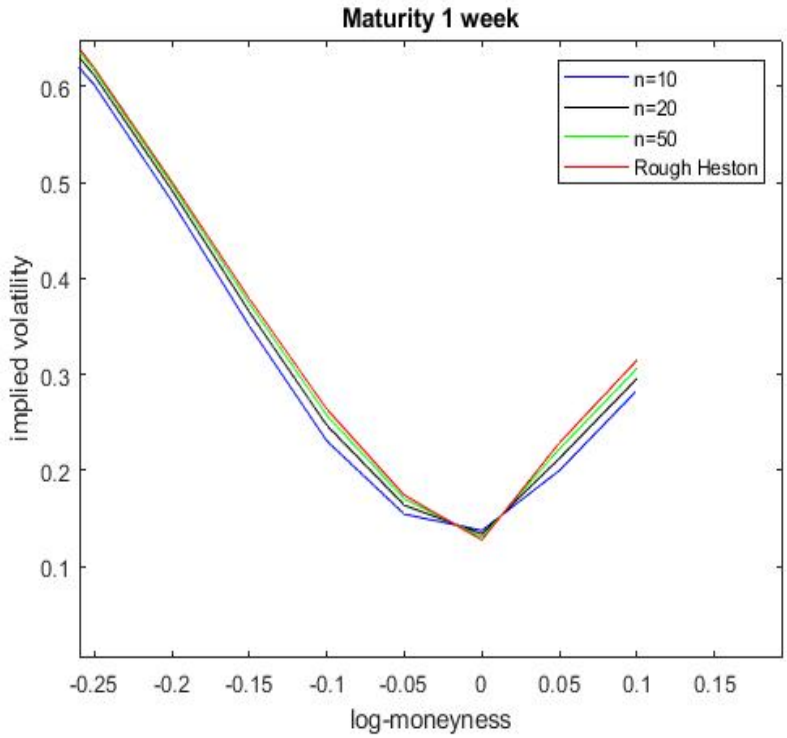

Figure 6.1: Comparison between the Lifted and the Rough model considering a different number of volatility factors when the time to maturity is one week

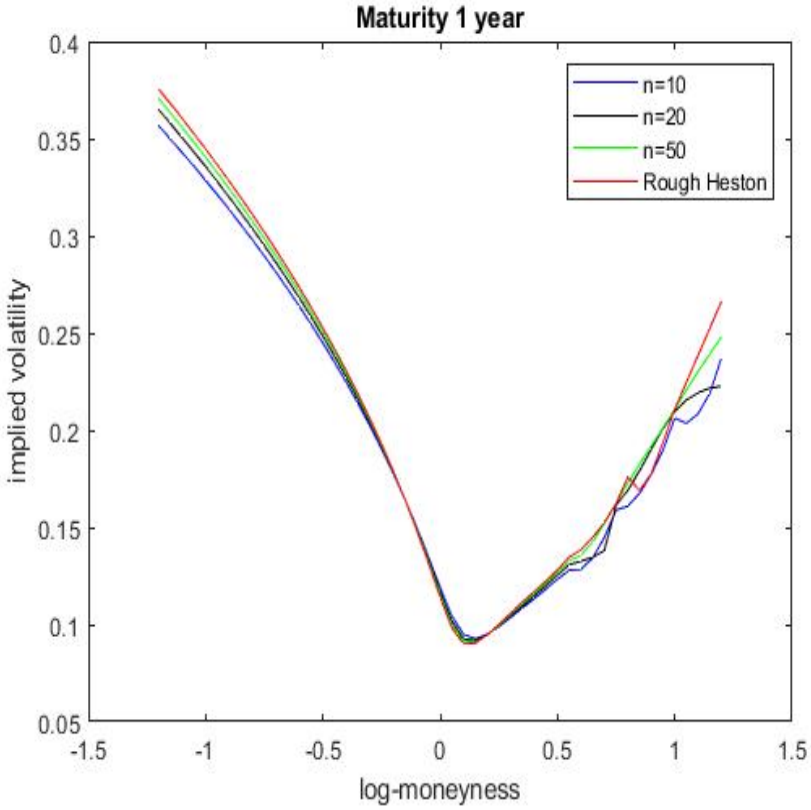

Figure 6.2: Comparison between the Lifted and the Rough model considering a different number of volatility factors when the time to maturity is one year

Tables 6.1 and 6.2 show the choice of the parameter r_n in accord to [3] and the quality of the approximation thanks to the Mean Squared Error (MSE) for the same times to expiry considered above.

	n	$r_n = 1 + 10n^{-0.9}$	MSE_{Price}	MSE_{vol}
Lifted Heston	10	2.26	1.7721e-08	1.7225e-02
	20	1.67	6.9630e-09	6.5956e-04
	50	1.3	1.2964e-09	1.6194e-04

Table 6.1: Lifted Heston model parameters and errors when T=1 week

	n	$r_n = 1 + 10n^{-0.9}$	MSE_{Price}	MSE_{vol}
Lifted Heston	10	2.26	2.9915e-07	1.4664e-04
	20	1.67	1.002e-07	1.0431e-04
	50	1.3	2.3463e-08	2.6583e-05

Table 6.2: Lifted Heston model parameters and errors when T=1 year

6.4.3 Computational time

Here we show how long the our algorithm takes to produces the graph presented in Figure 6.2. We consider 49 different strikes and one single maturity.

	n	$r_n = 1 + 10n^{-0.9}$	Time(seconds)
Lifted Heston	10	2.26	16.06
	20	1.67	17.22
	50	1.3	24.57
Rough Heston			50.28

Table 6.3: Lifted Heston computational time

Chapter 7

Conclusions

First, we resume the structure and the contents of this work.

Stochastic volatility models are able to capture the price movements on a short time scale. One of the most popular models among practitioners is the Heston model, which enjoys a closed form for the characteristic function. This feature allows fast pricing methods based on the Fourier transform.
However, the Heston model fails in reproducing the at-the-money skew of the implied volatility observed in the market.

In order to fit both the implied and the historical volatility, rough volatility models have been introduced. However, these models are no longer Markovian and the volatility process is no more a semi-martingale.

Recent works create the rough counterpart of the Heston model. Trasforming the Heston model time derivative in a fractional derivative, we can compute also the characteristic function in the rough framework.
The loss of the Markovian property leads to adopt the Adams-Bashforth-Moulton algorithm in order to solve the fractional derivative.

The introduction of the rough model is justified by the typical behaviors of the participants in high frequency markets. A microscopic model based on Hawkes processes, which are able to reproduce stylized facts observed in the market, is built. In the limit, the rough Heston model is obtained.

Since the Adams method requires a lot of resources to compute the fractional

derivative solution, we introduce the Lifted Heston model, a multi-factor approximation for the rough one.
Here, the variance process is built as a weighted sum of n factors driven by the same one-dimensonal Brownian motion.

The lifted model enjoys the best of the two worlds: it can reproduce precisely the ATM skew and it is Markovian. So, we can easily obtain the log-price characteristic function solving a finite system of ordinary Riccati equations.
This fact is translated in a remarkable speed up in the code execution, while the final result remains very accurate with respect to the rough model.

Table 7.1 resumes the differences between the tree models.

Characteristics	Heston	Rough Heston	Lifted Heston
Markovianity	✓	✗	✓
Semimartingale	✓	✗	✓
Fit short maturities skew	✗	✓	✓
Characteristic function	Closed	Fractional Riccati	n Riccati
Pricing	Fast	Slow	Fast

Table 7.1: Comparison between the three analyzed models

We conclude stating that, starting from the existing literature, this work analyzes in details the three models presented above, building an organic *Matlab* code which allows us to compare the three algorithms and to construct a realistic implied volatility surface in a reasonable computational time.

Appendix A

Main Codes

A.1 Pricing under Heston model

Call price

```
function P =
    Call_Price_Heston(S,K,T,r,kappa,theta,sigma,rho,V,alpha,L)

%%%%%%%%%%%%%%%%%%%%%%%%%%%%%%%%%%%%%%%%%%%%%%%%%%%%%%%%%%%%%%%%%%%%%%%%
% This function prices a Call option  with Maturity T and
% Strike K using the characteristic function of the price and
% Lewis' approach
%
% No FFT used
%
%
% INPUT:
% S : initial spot price
% r : risk free rate
% kappa,theta,sigma,rho : Heston model parameters
% V : initial vol in Heston model
% alpha : damping factor (alpha >0)
% L : truncation bound for the integral
%
%
% OUTPUT:
% P : European Call price
%
%%%%%%%%%%%%%%%%%%%%%%%%%%%%%%%%%%%%%%%%%%%%%%%%%%%%%%%%%%%%%%%%%%%%%%%%

```

```
25
26 %Heston characteristic function
27
28 b=@(nu)(kappa-1i*rho*sigma.*nu);
29 gamma=@(nu)(sqrt(sigma^2*(nu.^2+1i.*nu)+b(nu).^2));
30 a=@(nu)(b(nu)./gamma(nu)).*sinh(T*0.5.*gamma(nu));
31 c=@(nu)(gamma(nu).*coth(0.5*T.*gamma(nu))+b(nu));
32 d=@(nu)(kappa*theta*T.*b(nu)/sigma^2);
33
34 f=@(nu)(1i*(log(S)+r*T).*nu+d(nu));
35 g=@(nu)(cosh(T*
       0.5.*gamma(nu))+a(nu)).^(2*kappa*theta/sigma^2);
36 h=@(nu)(-(nu.^2+1i.*nu)*V./c(nu));
37
38 phi=@(nu)(exp(f(nu)).*exp(h(nu))./g(nu));
39
40
41 %function handle for the Fourier transform of the
42 %characteristic function
43 integrand=@(u)(real(phi(u-1i/2).*exp(1i*log(K)*u))./(u.^2+.25));
44
45 %explicit integration
46 II = integral(integrand,0,L);
47
48
49 % Lewis' Pricing formula
50 P = S - ((sqrt(S*K)*exp(-r*T/2)/pi)*II);
51
52 end
```

A.2 Pricing under rough Heston model

Call price

```
function [P] = Call_RoughHeston(S0,K,T,r,x)

%%%%%%%%%%%%%%%%%%%%%%%%%%%%%%%%%%%%%%%%%%%%%%%%%%%%%%%%%%%%%%%%%%%%%%%%%%%%
% This function prices a Call option using Lewis' approach and
% Adams' method for the characteristic function, considering
% the Rough Heston model for the volatility
%
%
% INPUT:
% S0 : initial spot price
% K : strike price
% T : time to expiry (in years)
% r : risk free rate
% x : Rough Heston parameters
%
%
% OUTPUT:
% P : European Call price
%
%%%%%%%%%%%%%%%%%%%%%%%%%%%%%%%%%%%%%%%%%%%%%%%%%%%%%%%%%%%%%%%%%%%%%%%%%%%%

%function handle for the Fourier transform of the
%characteristic function

integrand=@(u)(real(tr_fourier(x,T,u).*exp(i*log(K)*u)));

%explicit integration
II = integral(integrand,0,100);

%Lewis' Pricing formula
P = S0 - ((sqrt(S0*K)*exp(-r*T/2)/pi)*II);

end
```

Fourier trasform

```
function fii = tr_fourier(x,T,v)

%%%%%%%%%%%%%%%%%%%%%%%%%%%%%%%%%%%%%%%%%%%%%%%%%%%%%%%%%%%%%%%%%%%%%%%%%%%%
% This function computes the Fourier transform of the
% characteristic function for a vector of logstrike grid points
%
%
% INPUT:
% x: Heston models parameters
% T: options time to maturity (scalar)
% v: logstrike grid points
%
%
% OUTPUT:
% fii: Fourier transform of the characteristic function
%
%%%%%%%%%%%%%%%%%%%%%%%%%%%%%%%%%%%%%%%%%%%%%%%%%%%%%%%%%%%%%%%%%%%%%%%%%%%%

%Number of points in the log-strike grid
L=length(v);

%Initialization
CF=zeros(1,L);


%Computing the characteristic function for each log-strike
%grid point

for i=1:L
    CF(i)=phi(x,T,v(i)-1i/2);
end

%Computing the Fourier transform argument (Lewis' approach)
fii = CF./(v.^2+0.25);
end
```

Characteristic function (Adams' algorithm)

```
function [char_f] = phi(x,T,u)

%%%%%%%%%%%%%%%%%%%%%%%%%%%%%%%%%%%%%%%%%%%%%%%%%%%%%%%%%%%%%%%%%%%%%%%%%%%%
% This function computes the characteristic
% function for a logstrike grid point
%
%
% INPUT:
% x: Heston models parameters
% T: options time to maturity (scalar)
% u: logstrike grid point
%
%
% OUTPUT:
% char_f: characteristic function evaluated in u
%
%%%%%%%%%%%%%%%%%%%%%%%%%%%%%%%%%%%%%%%%%%%%%%%%%%%%%%%%%%%%%%%%%%%%%%%%%%%%

%Number of steps in the Adams scheme
N=1e3;
dt = T/N;

% rough Heston model parameters
nu = x(1);
Gamma= x(2);
rho = x(3);
theta = x(4);
V0 = x(5);
alpha = x(6);

% Fractional Riccati equation
F = @(v)(0.5*(-u.*u-1i*u) + Gamma.*(1i*u*rho*nu-1).*v +
    (0.5*(Gamma*nu*v).^2));

% Solution of fractional riccati equation with zero initial
% condition
y0 = 0;
y = zeros(1,N);

% Arrays containing the weights of the corrector and predictor
% formulas
a = zeros(1,N);
b = zeros(1,N);

```

```
% Coefficients computation
for k=1:N
    b(k) = (k^alpha - (k-1)^alpha);
    a(k) = (k+1)^(alpha+1) - 2*k^(alpha+1) + (k-1)^(alpha+1);
end

F0 = F(y0);
F_y = zeros(1,N);

% First step
p = b(1)*F0;
y(1) = ((dt^alpha)*(F(p)-(-alpha)*F0))/gamma(alpha+2);
F_y(1) = F(y(1));


% Corrector-predictor algorithm

for j=2:N
        p = ((dt^alpha)*(b(j)*F0+...
        sum((fliplr(b(1:j-1))).*F_y(1:j-1)))/...
        gamma(alpha+1);

        y(j) = (dt^alpha*(F(p)+((j-1)^(alpha+1)-(j-1-alpha)*...
        (j^alpha))*F0+sum((fliplr(a(1:j-1))).*F_y(1:j-1)))/...
        gamma(alpha+2);

        F_y(j) = F(y(j));
end

%Computing the first integral of the characteristic function
%with thetrapezoidal rule

% Trapezoidal weights
w = [0.5   ones(1,N-2)   0.5];
int1 = dt*(w*y');


% Adams weights

W=ones(1,N+1);

W(1)=(N-1)^(2-alpha)-(N-2+alpha)*N^(1-alpha);

W(2:N)=(N:-1:2).^(2-alpha)+(N-2:-1:0).^(2-alpha) -...
 2*(N-1:-1:1).^(2-alpha);
```

```
89
90 W=((dt)^(1-alpha)/gamma(3-alpha))*W;
91
92
93 % Fractional integral with trapezoidal rule
94 int2 = W(1:N+1)*[0;y'];
95
96 %Characteristic function
97 char_f = exp(theta*Gamma*int1+V0*int2);
98
99 end
```

A.3 Pricing under lifted Heston model

Call price

```
1  function [P] = Call_RoughHeston_MF(S0,K,T,r,x,n,r_n)
2
3  %%%%%%%%%%%%%%%%%%%%%%%%%%%%%%%%%%%%%%%%%%%%%%%%%%%%%%%%%%%%%%%%%%%%%%%%
4  % This function prices a Call option using Lewis' approach and
5  % Adams method for the characteristic function, considering
6  % the multi-factor Heston model for the volatility
7  %
8  %
9  % INPUT:
10 % S0 : initial spot price
11 % K : strike price
12 % T : time to expiry (in years)
13 % r : risk free rate
14 % x : nu,lambda,rho,theta,V0,alpha
15 %     Rough Heston parameters
16 % n: number of factors
17 % r_n: multifactor coefficient
18 %
19 %
20 % OUTPUT:
21 % P : European Call price
22 %
23 %%%%%%%%%%%%%%%%%%%%%%%%%%%%%%%%%%%%%%%%%%%%%%%%%%%%%%%%%%%%%%%%%%%%%%%%
24
25
26
27
```

```
%function handle for the Fourier transform of the
%characteristic function
integrand=@(u)(real(tr_fourier_MF(x,T,u,n,r_n).*...
exp(i*log(K)*u)));

%explicit integration
II = integral(integrand,0,100);

%Lewis' Pricing formula
P = S0 - ((sqrt(S0*K)*exp(-r*T/2)/pi)*II);

end
```

Fourier trasform

```
function fii = tr_fourier_MF(x,T,v,n,r_n)

%%%%%%%%%%%%%%%%%%%%%%%%%%%%%%%%%%%%%%%%%%%%%%%%%%%%%%%%%%%%%%%%%%%%%%%%%%%%
% This function computes the Fourier transform of the
% characteristic function for a vector of logstrike grid points
%
%
% INPUT:
% x: Heston models parameters
% T: options time to maturity (scalar)
% v: logstrike grid points
% n: number of factors
% r_n: multifactor coefficient
%
%
% OUTPUT:
% fii: Fourier transform of the characteristic function
%
%%%%%%%%%%%%%%%%%%%%%%%%%%%%%%%%%%%%%%%%%%%%%%%%%%%%%%%%%%%%%%%%%%%%%%%%%%%%

%Number of points in the log-strike grid
L=length(v);

%Initialization
CF=zeros(1,L);

%Computing the characteristic function for each log-strike
%grid point
for i=1:L
    CF(i)=phi_LH(x,T,v(i)-1i/2,n,r_n);
```

```
end

%Computing the Fourier transform argument (Lewis' approach)
fii = CF./(v.^2+0.25);
end
```

Characteristic function (Multi-factor approach)

```
function [L_n] = phi_LH(x,T,u,n,r_n)

%%%%%%%%%%%%%%%%%%%%%%%%%%%%%%%%%%%%%%%%%%%%%%%%%%%%%%%%%%%%%%%%%%%%%%%%%%%%
% This function computes the the characteristic function for a
% log-strike grid point following the Multifactor approach
%
%
% INPUT:
% x: Heston models parameters
% T: options time to maturity (scalar)
% u: logstrike grid point
% n: number of factors
% r_n: multifactor coefficient
%
%
%
% OUTPUT:
% char_f: characteristic function evaluated in u
%
%%%%%%%%%%%%%%%%%%%%%%%%%%%%%%%%%%%%%%%%%%%%%%%%%%%%%%%%%%%%%%%%%%%%%%%%%%%%

% rough Heston model parameters
nu = x(1);
lambda= x(2);
rho = x(3);
theta = x(4);
V0 = x(5);
alpha = x(6);

% Fractional Riccati equation
u=1i*u;
F = @(v)(0.5*(u.*u-u) + (u*rho*nu-lambda).*v + (0.5*(nu*v).^2));

% Multifactor model coefficients
i=[1:n];
c=((r_n^(1-alpha)-1)*(r_n^((alpha-1)*(1+n/2)))*...
      (r_n.^((1-alpha).*i)))/(gamma(alpha)*gamma(2-alpha));
```

```
x=((1-alpha)*(r_n^(2-alpha)-1)*(r_n.^(i-1-n/2)))/...
      ((2-alpha)*(r_n^(1-alpha)-1));


%% Computing phi

%Initialization
N_times=2e2; %number of points on the time grid
dt=T/N_times;
phi=zeros(n,N_times+1);

for k=1:N_times
          phi(:,k+1)=((ones(n,1)./(ones(n,1)+dt.*x')).*(phi(:,k)...
              +dt*F(c*phi(:,k))));
end


% Here we propose three different methods in order to compute
% g_n. One method is the analytical integration, one is the
% numerical integration with the trapezoidal rule and the last
% is the formula obtained solving the integral by hand. We
% obtain the same result in the tree different cases, but the
% last one is the fastest.
%
% Notice that the last method can be used only if theta is a
% constant (our assumption)
%
%
%
%% Computing g_n explicitly
%
% int1=zeros(n,N_times);
% time=linspace(0,T,N_times);
%
% for i=1:N_times
%    integrand=@(s) exp(-x.*(time(i)-s));
%    int1(:,i)=integral(integrand,0,time(i),'ArrayValued',true);
% end
%
% g_n=V0.*ones(1,N_times)+theta*lambda*(c*int1);
%
%
%% Computing g_n with trapezoidal rule
% W=dt*ones(1,N_times);
%
```

```
% DT=[1:N_times]*dt;
%
% int1=(c*exp(-x'*DT)).*W;
% g_n=V0+theta*lambda*int1;

%% Computing g_n by hand
DT=[0:N_times]*dt;

int1=(c./x)*(1-exp(-x'*DT));
g_n=V0+theta*lambda*int1;

%% Computing the characteristic function in each time grid node
int2=F(c*phi).*flip(g_n);

% Trapezoidal rule weights
W=dt*ones(1,N_times+1);
W(1)=0.5*dt;
W(end)=0.5*dt;

L_n=exp(int2*W');

 end
```

A.4 Comparing classic and lifted Heston

Characteristic function with n=1

```
function [L_n] = phi_LvsH(x,T,u)

%%%%%%%%%%%%%%%%%%%%%%%%%%%%%%%%%%%%%%%%%%%%%%%%%%%%%%%%%%%%%%%%%%%%%%%%%%%%
% This function computes the the characteristic function for a
% logstrike grid point following the rough Heston Multifactor
% approach. These function has been produce in order to
% compare the multi-factor approach with n=1 and the classical
% Heston model.
%
%
% INPUT:
% x: Heston models parameters
% T: options time to maturity (scalar)
% u: logstrike grid point
%
%
```

```
% OUTPUT:
% char_f: characteristic function evaluated in u
%
%%%%%%%%%%%%%%%%%%%%%%%%%%%%%%%%%%%%%%%%%%%%%%%%%%%%%%%%%%%%%%%%%%%%%%%%%%%%

% rough Heston model parameters
nu = x(1);
Gamma= x(2);
rho = x(3);
theta = x(4);
V0 = x(5);
alpha = x(6);

% Fractional Riccati equation
u=1i*u;
F = @(v)(0.5*(u.*u-u) + (u*rho*nu-Gamma).*v + (0.5*(nu*v).^2));

% Multifactor model coefficients when n=1
c=1;
x=0;


%% Computing phi

%Initialization
N_times=1e3; %number of points on the time grid
dt=T/N_times;
phi=zeros(1,N_times);

for k=1:N_times-1
        phi(k+1)=((1/(1+dt*x')).*(phi(k)+dt*F(c*phi(k))));
end


%% Computing g_n with trapezoidal rule

% Trapezoidal rule weights
W=dt*ones(1,N_times);
W(1)=0.5*dt;
W(end)=0.5*dt;

DT=[1:N_times]*dt;

% We deal only with 2 coefficients in the multi-factor
% approach. The only way we can can choose in order to compute
```

```
% g_n is the trapezoidal rule

int1=(c*exp(-x'*DT)).*W;
g_n=V0+theta*Gamma*int1;

%% Computing the characteristic function in each time grid node
int2=F(c*phi).*flip(g_n);

L_n=exp(int2*W');

 end
```

Appendix B

Calibration and Future Developments

In order to go deep with the numerical analysis, we also try to create a calibration algorithm. Obviously, we worked with the functions we used to price options in the rough and in the lifted frameworks.

We can follow two approaches when we deal with the calibration: we can calibrate on option prices or on the implied volatility. Obviously, the goal of the algorithm is to minimize the difference between the prices observed in the market and the one obtained from the calibrated parameters.
However, the two approaches didn't lead us to significantly different results and what we will say in the following paragraphs holds true for both cases.

In order to design our algorithm we analyze three different *Matlab* functions: *lsqnonlin*, *fminsearch*, *fmincon*. In each case, the designed algorithms have to minimize the square norm of the difference between calibrated and "real" prices. What we called "real" prices are option prices that we artificially obtain from the rough Heston algorithm. In order to find the calibrated prices, we use the Lifted Heston with $n = 20$.
Going back to *Matlab* algorithms, we decide to discard *fmincon* because it takes too long time to generate results. *lsqnonlin* is the fastest function in this group, but despite of this it is not very accurate. The only function that provide a good trade-off between computational time and results precision is *fminsearch*. Our brief analyses is based on this function.

Recall that, while the rough model has 6 parameters, the Lifted Heston has 7 parameters. Fixing n, the additional parameter r_n doesn't need to be calibrated. So, from now, we consider the vector $(V_0, \theta, \gamma, \nu, \rho, H, r_n)$.

Because of the difficulties encountered, we only talk about a single-parameter calibration.
It was not possible to calibrate γ and ν and we were not able to provide interesting results. *fminsearch*, instead, works well when we deal with H, V_0, θ and ρ.

The main problem we encountered is the fact that our algorithm works only when the the option is at-the-money or near. We obtained meaningful parameters only when the log-moneyness k respect the constraint $-0.1 < k < 0.1$. If we consider a different part of the surface, we are not able to find the minimum of the norm and this translates in the fact that a lot of prices are not a number.

In the future, it can be interesting to go deep with the calibration algorithm, extending it to the whole volatility surface. Maybe it can be possible to create a multi-parameters calibration.
Another possible development is to analyze why our algorithm doesn't work when we deal with certain parameters.

We decide not to include our calibration algorithm because it contains some errors and it works only on a self-constructed case.

Bibliography

[1] K. Diethelm, N.J. Ford, A.D. Freed. A Predictor-Corrector Approach for the Numerical Solution of Fractional Differential Equations. *https://doi.org/10.1023/A:1016592219341*, 2002

[2] M. Fukasawa. Asymptotic analysis for stochastic volatility: Martingale expansion. *Finance and Stochastics*, 15(4):635-654, 2011.

[3] E. Abi Jaber. Lifting the Heston model. *arXiv:1810.04868v2*,2019

[4] T. Jaisson, M Rosenbaum. Limit theorems for nearly unstable Hawkes processes. *https://doi.org/10.1214/14-AAP1005*, 2015

[5] F. Comte, E. Renault. Long memory in continuous-time stochastic volatility models. *Mathematical Finance*, 8(4):291–323, 1998

[6] E. Abi Jaber, O. El Euch. Multi-factor approximation of rough volatility models. *arXiv:1801.10359v3*, 2018

[7] M. Schmelzle. Option pricing formulae using Fourier transform: Theory and application. 2010

[8] T. Jaisson, M Rosenbaum. Rough fractional diffusions as scaling limits of nearly unstable heavy tailed Hawkes processes. *arXiv: 1504.03100v1*, 2015

[9] O. El Euch, M. Rosenbaum. The characteristic function of rough Heston model. *https://doi.org/10.1111/mafi.12173*, 2016

[10] O. El Euch, M. Fukusawa, M. Rosenbaum. The microstuctural foundations of leverage effect and rough volatility. *https://doi.org/10.1007/s00780-018-0360-z*, 2016

[11] J. Gatheral, T. Jaisson, M. Rosenbaum. Volatility is rough. *arXiv:1410.3394v1*, 2014.